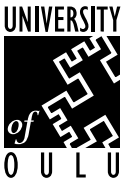

DEGREE PROGRAMME IN WIRELESS COMMUNICATIONS ENGINEERING

MASTER'S THESIS

PERFORMANCE OF DELAY CONSTRAINED MULTI-USER NETWORKS UNDER BLOCK FADING CHANNELS

Author _____
Mohammad Shehab

Supervisor _____
Prof. Matti Latva-aho

Second examiner _____
Dr. Hirley Alves

Accepted _____ /_____ 2017

Grade _____

Shehab M. (2017) Performance of delay constrained multi-user networks under block fading channels. Department of Communications Engineering, University of Oulu, Oulu, Finland. Master's thesis, 50 p.

ABSTRACT

Effective Capacity (EC) indicates the maximum communication rate subject to a certain delay constraint while the effective energy efficiency (EEE) is the ratio between this EC and power consumption. In this thesis, we analyze the EC and EEE of multi-user networks operating in the finite blocklength (FB) regime. We consider a layout in which a number of users communicate through a common controller. A closed form approximation for the per-user EC is obtained in Nakagami-m fading collision channels. The interference between transmitted data packets degrades the EC of each user. We analyze this decrease proposing three methods to alleviate the interference effect for one of the users namely power control, delay relaxation and joint compensation. Our results show that systems with stringent delay constraints favor power controlled compensation while for shorter packets, the amount of compensation needed by both θ relaxation and power increases is higher. Thus, it is more costly to compensate networks transmitting shorter packets. For the hybrid method, we maximize an objective function whose parameters are determined according to the design priorities (e.g. rate and latency requirements). Results reveal that there is a unique throughput maximizer which is obtained at an intermediate operational point applying both power control and delay relaxation in the joint compensation process. Furthermore, we characterize the per-user EEE for different power consumption models. The results show that accounting for empty buffer probability enhances the per-user EEE. Considering flexible transmission power and extending the maximum delay tolerance boosts the per-use EEE which is depicted in the thesis as well.

Keywords: Finite blocklength, Effective capacity, Effective energy efficiency, Multi-user interference, Machine-to-machine communication.

Shehab M. (2017) Suorituskyvyn analysointi viiverajoitetussa usean käyttäjän verkossa lohkohäipyvissä kanavissa. Oulun yliopisto, sähkö- ja tietotekniikan osasto. Diplomityö, 50 s.

TIIVISTELMÄ

Efektiivinen kapasiteetti kertoo suurimman tietoliikenteen datanopeuden määritetyillä viiverajoituksilla, kun taas efektiivinen energiatehokkuus on efektiivisen kapasiteetin ja tehonkulutuksen suhde. Tässä diplomityössä analysoidaan efektiivistä kapasiteettiä ja efektiivistä energiatehokkuutta monisolmuverkoissa, kun käytetään äärellistä lohkon pituutta. Työssä käytetään mallia, jossa tietty määrä käyttäjiä kommunikoi yhteisen kontrolliyksikön ohjaamana. Käyttäjäkohtaisen efektiivisen kapasiteetin approksimaatio datapakettien törmäyksiä mallintavassa Nakagami-m ?häipyvässä kanavassa esitetään suljetussa muodossa. Lähetettyjen pakettien välinen häiriö pienentää kunkin käyttäjän efektiivistä kapasiteettia. Tätä ilmiötä pyritään lieventämään kolmella ehdotetulla menetelmällä eli tehonsäädöllä, viiveen relaksoinnilla ja näiden yhdistelmällä. Tutkimustulokset osoittavat, että tiukkojen viiverajoitusten voimassa ollessa tehopohjainen kompensointi toimii parhaiten kun taas lyhyille paketeille vaaditaan molempia menetelmiä. Niinpä lyhyitä paketteja lähettävien verkkojen kompensointimenetelmät ovat kalliita. Hybridimenetelmässä maksimoidaan kohdefunktio, jonka parametrit määritellään suunnittelukriteerien mukaan (esim. datanopeus- ja viivevaatimukset). Tulokset paljastavat, että löytyy yksittäinen verkon läpäisykyvyn maksimoiva keskialueen toimintapisteen kohta teho- ja viivepohjaista kompensointia yhdessä käytettäessä. Lisäksi työssä mallinnetaan solmukohtaista efektiivistä energiatehokkuutta eri tehonkulutusmalleilla. Tulokset osoittavat, että eityhjän puskurin todennäköisyyden huomioon ottaminen parantaa käyttäjäkohtaista efektiivistä energiatehokkuutta. Työssä kuvataan myös, että joustavan lähetystehon käyttö yhdessä väljennetyn maksimiviivetoleranssin kanssa parantaa efektiivistä energiatehokkuutta.

Avainsanat: äärellinen lohkon pituus, efektiivinen kapasiteetti, efektiivinen energiatehokkuus, monikäyttöhäiriö, laitteiden keskinäinen kommunikaatio

TABLE OF CONTENTS

FOREWORD

The focus of this thesis is to study reliable transmission of short packets in multi-user environments. This research was carried out at Center for wireless communication (CWC) as part of 5Gto10G project and was partially supported by Finnish Funding Agency for Technology and Innovation (Tekes), Huawei Technologies, Nokia and Anite Telecoms. I would like to express my sincere gratitude to Dr. Hirley Alves for his guidance, and immense knowledge. I would like to thank Prof. Matti Latva-aho for giving me the opportunity to join the research group in the CWC. Special thanks to my family who supported me all the time and above all to God who led me to this achievement.

ABBREVIATIONS AND SYMBOLS

AWGN	Additive White Gaussian Noise
bpcu	bit per channel use
CSI	Channel State Information
ICSI	Imperfect Channel State Information
EC	Effective Capacity
EEE	Effective Energy Efficiency
FB	Finite Blocklength
KKT	Karush-Kuhn-Tucker
LoS	Line of Sight
LTE	Long Term Evolution
max	maximize
NBP	Non-empty Buffer Probability
PDF	Probability Density Function
QoS	Quality Of Service
SINR	Signal-to-Interference-plus-Noise Ratio
SNR	Signal to Noise Ratio
s.t	subject to
UR	Ultra Reliable
URC	Ultra Reliable Communication
5G	fifth mobile generations

$C(\rho)$	Shannon capacity
D_{max}	maximum delay
$E[]$	expectation of
EC	effective capacity
EC_{max}	maximum effective capacity
EC_{Ry}	effective capacity in Rayleigh channel
$\mathfrak{L}(\epsilon, \lambda)$	Lagrangian function
N	number of users
$Pr()$	probability of
P_c	power dissipated in circuit
P_{max}	maximum transmission power
P_{nb}	non-empty buffer probability
P_{out_delay}	delay outage probability
$P_t(\rho)$	power consumption
$Q(x)$	Gaussian Q-function
$Q^{-1}(x)$	inverse Gaussian Q-function
$R(T_f, \epsilon)$	coding (achievable) rate
T_f	blocklength
$V(\rho)$	channel dispersion

e	exponential Euler's number
$\|h\|^2$	fading coefficient
$\log$	natural logarithm to the base e

$\log_2$	logarithm to the base 2
m	fading parameter
r	normalized achievable rate
r_f	fixed rate
r_f^*	optimum fixed rate
$f_z(z)$	fading parameter probability density function
r_i	normalized achievable rate in multi-user network
$\mathbf{w}$	additive while Gaussian noise vector
$\mathbf{x}_n$	transmitted signal vector of user n
$\mathbf{y}_n$	received signal vector of user n
z	fading random variable

α	collision loss factor
α_c	compensation loss factor
α_{c_o}	operational point of compensation loss factor
α_t	total loss
γ_c	compensation gain
θ	delay exponent
ϵ	error probability
ϵ_t	target error probability
ϵ^*	optimum error probability
ζ	inverse drain efficiency
η_α	compensation loss priority factor
η_θ	delay priority factor
λ	Lagrangian multiplier
μ	arrival rate
ρ	signal to noise ratio
ρ_c	compensation SNR
ρ_{c_o}	operational point of compensation SNR
ρ_i	signal-to-interference-plus-noise ratio
ρ_s	SINR of other non-compensating users

1. INTRODUCTION

Modern communication systems have become an indispensable part of our daily lives. In such systems, information bits are usually transmitted through non ideal channels in the form of coded packets. For a certain communication channel, Shanon capacity [1] is defined as the rate by which information can be transmitted error free. Conventionally, communication systems are designed based on Shanon theory, which resorts to long data package transmission when there is a large number of channel uses per packet. However, recently introduced applications such as vehicle to vehicle communication, and smart grids have a massive number of users that use short messages to communicate to each other. Transmission of such short packets is not liable to Shannon capacity anymore as Shannon theory performs poorly at finite blocklengths (FB) [2]. Instead, the maximum transmission rate of FB packets was characterized in [3], and shown to be a function not only of the signal to noise ratio (SNR), but also blocklength and maximum error probability.

Applications which use short messages usually have strict delay constraints where packets are required to be transmitted with minimum latency and a high level of reliability [4], which is not easily achieved using conventional coding with long blocklength. Often real time applications (e.g. Internet of things [5] [6] [7] [8] and industrial automation) require a fast response time with minimum delay, in the order of a few milliseconds. The next generation of mobile communication, namely 5G [9] [10] [11], will support such demands via machine type communications [12] [13] [14] [15]. In this context, ultra reliable communication (URC) has emerged to provide solutions for reliable and low latency transmissions [4], [16] [17], and FB codes are a promising solution to achieve such goals as envisaged by [2].

Communication in the FB regime has gained an increasing attention in the recent years [2, 3, 4, 16, 18, 19, 20, 21, 22, 23, 24]. The maximum transmission rate of FB packets was characterized in [3], [18], where Wang et al. characterized the attainable rate as a function of blocklength and error probability ϵ for block fading channels. The results highlighted a constant gap between their achievability bound and turbo code rates in LTE-Advanced. In [19], a per-user throughput model was introduced for additive white Gaussian noise (AWGN) and quasi-static collision channels where interference is treated as additive Gaussian noise while considering average delay. The effect of relaying of blocklength-limited packets was studied and compared to direct transmission in [20], [21] where the authors concluded that relaying is more efficient than direct transmission in the FB regime specially with average channel state information (CSI). Recently, in [22], Schiessl et al. studied the performance of FB communication with imperfect channel state information (ICSI). Automatic repeat request [25] [26] and resource allocation schemes [27] were also discussed in order to raise reliability.

Effective capacity (EC) was introduced in [28] as a metric that guarantees certain quality requirements by capturing the physical and link layers aspects [29] [30]. It provides an indication of the maximum possible arrival rate that can be supported by a network subject to a particular latency requirement. A finite blocklength statistical model for a single user effective rate in bits per channel use (bpcu) for a certain error probability with quality of service (QoS) exponent was discussed in [3] and [23] for Rayleigh block fading channels, where the channel is assumed to be fixed for a block of T_f symbols. However, a closed form expression for the effective rate (or capacity) was

not provided in these discussions. Musavian et al. analyzed the EC maximization of secondary user with some interference power constraints for primary user in a cognitive radio environment [31]. Three types of constraints were characterized namely average interference power, peak interference power and interference power outage. To the best of our knowledge, no one has addressed the EC analysis and maximization for FB packets transmission in multi-users collision scenario.

Effective energy efficiency (EEE) is defined as the ratio between EC and the total consumed power [32]. The maximization of EEE is of great importance for energy limited systems such as sensor networks and massive machine-to-machine networks [33] where the goal is to maximize the throughput for each consumed unit of power. In [34], empty buffer probability was considered as an EEE booster for long packets transmission. The trade off between EEE and EC was highlighted in [35] where the authors suggested an algorithm to maximize the EC subject to EEE constraint but without considering probability of transmission error that appears in finite blocklength communication due to imperfect coding. She et al. showed in [36] that the relation between EEE and delay in wireless systems is not always a tradeoff. They illustrated that a linear relation between service rate and power consumption leads to an EEE-delay non-tradeoff region.

1.1. Thesis contribution

In this thesis, we analyze multiuser throughput of short packet transmission in quasi-static Nakagami-m fading channels under delay exponent limit, which is directly linked to the delay outage probability. A closed form approximation for the per-user EC is obtained which leads us to characterize the effect of collision on the system performance for different fading environments such as Rayleigh and Ricean fading. After that, we focus on Rayleigh fading proposing three methods to allow one of the users recover from this interference effect: *i*) Compensation via power control; *ii*) compensation via delay relaxation; and *iii*) hybrid of power control and delay relaxation. Power controlled compensation depends on increasing the power of a certain user instantly to recompense for the interference resulting from the other users towards this user. This does have a side effect on the other users in the system as this power increase would cause more interference to them. We study this impact where the results show that the side effect of power controlled compensation appears to be worse for less stringent delay constraints, while it is more convenient to employ delay relaxation in the case of longer packets. Furthermore, we illustrate the trade off between the above two procedures, then we introduce a hybrid model which combines both of them. The operational point to determine the amount of compensation performed by each of the two methods in the hybrid model is determined by means of an objective function leveraging the system performance.

Furthermore, based on the per-user EC work, we extend the analysis to the per-user EEE in multi-user networks communicating in the FB regime. First, we prove that the power consumption model accounting for the probability of empty buffer which was introduced in [34] is valid as well for blocklength limited packets. Then, we emphasize that considering the probability of emptying the buffer during transmission of short packets boosts the per-user EC and EEE when compared to the case when the

buffer is always full. Finally, we confirm the fact that flexible transmission power and extending the allowable delay provides EEE gain over fixed transmission power.

1.2. Thesis Outline

The rest of the thesis is organized as follows: in Chapter 2, we define communication at FB, effective capacity and energy efficiency. In Chapter 3, we obtain a closed form expression of the per-user EC for multi-users in Nakagami-m collision channels and characterize the optimum error probability which maximizes the EC. After that, in Chapter 4, we analyze the effect of interference on the EC of each user compared to the single user scenario and how to compensate for it. In Chapter 5, we discuss the per-user EEE in the finite blocklength regime considering empty buffer probability. Finally, we state the thesis conclusions and suggested future work in Chapter 6.

2. PRELIMINARIES

The focus of this thesis lies on studying the performance of multi-node networks communicating with short messages and with limited delay bounds. Our performance metrics are the effective capacity (EC) and the effective energy efficiency (EEE). We study how different network parameters such as delay outage probability, blocklength, transmission power, and probability of decoding error affect these metrics in trade-off with each other. In this chapter, we start by stating some definitions and highlight related work.

2.1. Communication at finite blocklength

2.1.1. Single node scenario

We start by presenting the notion of FB transmission in which short packets are conveyed at rate that depends not only on the SNR, but also on the blocklength T_f given in the unit of "symbol periods", and the probability of error ϵ [2]. In this case, ϵ has a small value but not vanishing. For error probability $\epsilon \in [0, 1]$ and a signal to noise ratio equals to ρ, the maximal coding rate for various channels in the finite blocklength regime is given by

$$R^*(T_f, \epsilon) = C(\rho) - \sqrt{\frac{V(\rho)}{T_f}} Q^{-1}(\epsilon) + \frac{\log_2 T_f}{2T_f}, \tag{1}$$

where $Q(x) = \int_0^\infty \frac{1}{\sqrt{2\pi}} e^{\frac{-t^2}{2}} dt$ is the Gaussian Q-function, $C(\rho)$ is the Shannon limit for long packets and $V(\rho)$ is the channel dispersion. The Capacity $C(\rho)$ and the channel dispersion for AWGN channels are given by

$$C(\rho) = \log_2(1 + \rho), \tag{2}$$

$$V(\rho) = \rho \frac{2 + \rho}{(1 + \rho)^2} (\log_2(e))^2. \tag{3}$$

The relationship between the transmission rate R and error probability ϵ shows that R is increasing in ϵ because the inverse Q-function $Q^{-1}(\epsilon)$ is a decreasing function in ϵ. This means that by allowing higher error probability, we can transmit with a higher rate. This may be applicable in some streaming application where high reliability is not a critical issue (e.g football match streaming). The maximal coding $R^*(T_f, \epsilon)$ rate is expected to reach an asymptotic value of C as the packet length T_f approaches ∞.

In Fig. 2.1, we give a normalized plot for the relation between the capacity and achievable rate of finite short packets for AWGN channel as $\epsilon = 10^{-3}$ and $\rho = 1$. We notice that the normalized achievable rate increases with the packet length T_f till reaching the capacity $C(\rho)$ at infinite blocklength. We conclude that at blocklength $T_f < 1000$ symbol periods, the achievable rate is less than 90% of the capacity and hence Shannon limit is not accurate in this case.

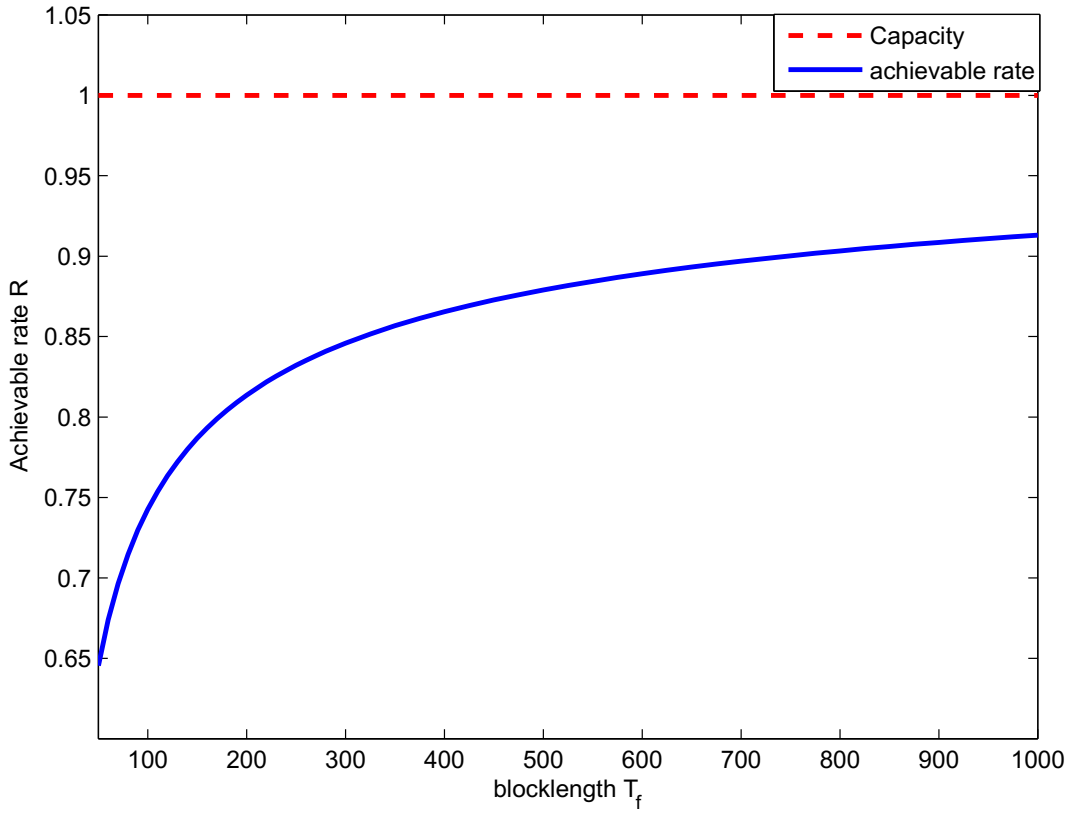

Figure 2.1. Normalized achievable rate $R(T_f, \epsilon)$ vs the packet length T_f for AWGN channel with parameters $\epsilon = 10^{-3}$ and $\rho = 1$.

For block fading channels, the achievable rate expression is affected by the fading coefficient and the normalized achievable rate in bits per channel use (bpcu) is given by

$$r = \log_2(1 + \rho|h|^2) - \sqrt{\frac{1}{T_f}\left(1 - \frac{1}{(1+\rho|h|^2)^2}\right)}Q^{-1}(\epsilon)\log_2(e), \tag{4}$$

where $|h|^2$ is the channel fading coefficient, whose PDF is denoted as $f_z(z)$.

2.2. Effective capacity

The concept of EC indicates the capability of communication nodes to exchange data with maximum rate and certain latency constraint. A statistical delay violation model implies that an outage occurs when a packet delay exceeds a maximum delay bound D_{max}. The delay outage probability is defined as [**?**]

$$P_{out\_delay} = \Pr(delay \geq D_{max}) \approx e^{-\theta.EC.D_{max}}, \tag{5}$$

where $\Pr(\cdot)$ denotes the probability of a certain event. Conventionally, a system's tolerance to long delay is measured by the delay exponent θ. The system tolerates

large delays for small values of θ (i.e., $\theta \to 0$) while for large values of θ, it becomes more delay strict. For example, a system with unity EC and a delay outage probability $P_{out\_delay} = 10^{-3}$ can tolerate a maximum delay $D_{max} = 691$ symbol periods for $\theta = 0.01$ and 23 symbol periods when $\theta = 0.3$.

In quasi-static fading, the channel remains constant within each transmission period T_f [21], and the EC in bits per channel use (bpcu) is [23]

$$EC(\rho, \theta, \epsilon) = -\frac{1}{T_f \theta} \log \left(E_{z=|h|^2} \left[\epsilon + (1-\epsilon) e^{-T_f \theta r} \right] \right), \tag{6}$$

where r is given in 4 In [3, 23], the effective capacity is statistically studied for single node scenario, but never to a closed form expression. It has been proven that the EC is concave in ϵ and hence, has a unique maximizer. Here, we present a part of the results discussed in [23]. Also, as the delay constraint θ becomes higher (i.e, more strict), the EC decreases as appears from (6). In Figure 2.2, we plot the EC vs error probability ϵ for different values of delay constraint θ to depict the EC-θ trade-off. The figure shows that when the delay constraint becomes more strict (has higher value), the EC decreases and vice versa. The figure also shows the concavity of EC in ϵ where ϵ has a unique optimum value which maximizes the EC in each curve. Later in the thesis, we define the optimum value of error probability ϵ^* analytically.

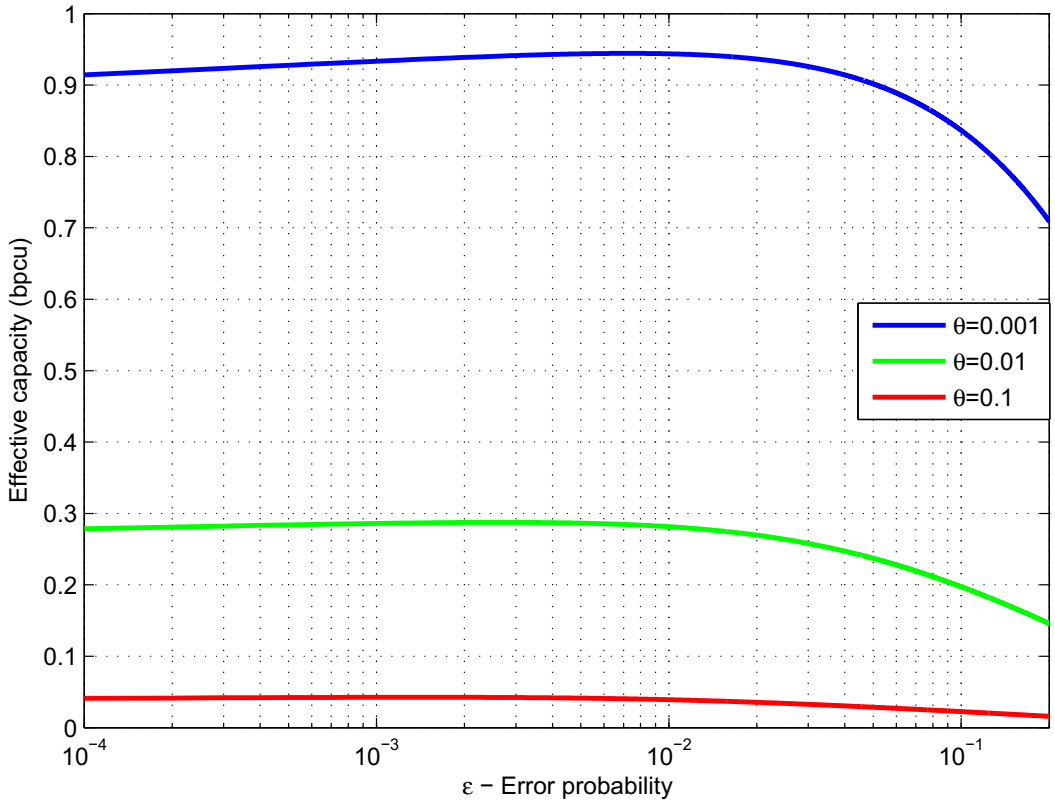

Figure 2.2. Effective capacity vs error probability ϵ for different values of θ in Rayleigh fading where $\rho = 2$, $T_f = 1000$.

In some applications, it is more efficient to transmit with a invariable rate or the transmitter does not have enough channel information and hence, unable to adapt its transmission rate to the channel conditions. In contrary to flexible rate transmission where the rate depends on fading conditions, the normalized achievable rate is kept at a fixed value r_f while the probability of error becomes variable and is defined as

$$\epsilon = Q\left(\frac{\log_2(1+\rho|h|^2) - r_f}{\sqrt{\frac{1}{T_f}\left(1-\frac{1}{(1+\rho|h|^2)^2}\right)\log_2 e}}\right). \tag{7}$$

In Fig. 2.3, we compare the EC vs the delay constraint θ for fixed and variable rate transmissions. The SNR and the blocklength are set as $\rho = 1$, and $T_f = 1000$, respectively. It can be observed that for high values of θ, fixed rate transmission performs strictly better. The figure also confirms the fact that EC is monotonically decreasing in θ where the EC degrades with the increase of delay constraint θ.

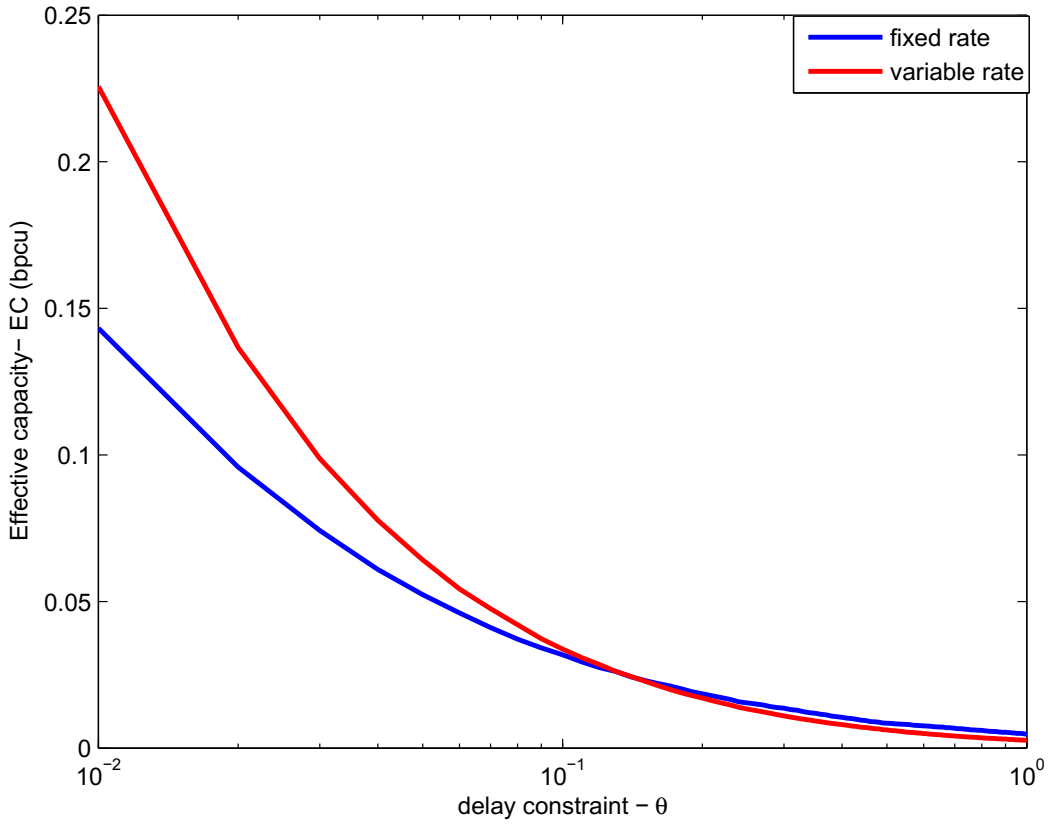

Figure 2.3. Comparison between fixed rate transmission and variable rate for different values of delay constraint θ where $\rho = 1$, and $T_f = 1000$.

Also in [23], the EC has been shown to be concave in r_f and hence the EC has a unique fixed rate maximizer. The fixed rate has the same behavior as EC with the delay constraint θ where increasing the value of θ (i.e more stringent delay constraint)

degrades the transmission rate. Fixed rate also have a unique maximum value r_f^* which will be determined analytically in the next chapter.

2.3. Effective energy efficiency

Defined as the ratio between EC and consumed power, the EEE metric indicates the network's capability of achieving a certain latency restricted rate with minimum energy consumption [37]. Here, we characterize the EEE in FB regime for different power models. Consider the model in which power consumption is defined by

$$P_t(\rho) = \zeta\rho + P_c \tag{8}$$

with ζ being the inverse drain efficiency of the transmit amplifier and P_c the hardware power dissipated in circuit [34].

In [34], empty buffer probability was considered for long packet transmission where the service process is defined by Shannon limit $C = \log(1+\rho z)$ where it was proven that this model is valid as an energy consumption model for long packets. In this section, we show the effect of EEE maximization with empty buffer probability and compare it with the case of always full buffer for single node scenario in Rayleigh fading channels as z is an exponential random variable modeling the Rayleigh fading channel. After accounting for the non-empty buffer probability, the power consumption is formulated as

$$P_t(\rho) = \zeta P_{nb}\rho + P_c = \frac{\mu}{E_z\left[\log(1+\rho z)\right]}\zeta\rho + P_c, \tag{9}$$

with $P_{nb} = \frac{\mu}{C}$ denoting the non-empty buffer probability (NBP), and μ denoting the data arrival rate. Notice that here the noise is normalized so that the SNR ρ frankly represents the transmit power. The corresponding EEE is

$$EEE = \frac{-\frac{1}{\theta}\log E_z\left[\log(1+\rho z)^{-\theta}\right]}{\frac{\mu}{E_z[\log(1+\rho z)]}\zeta\rho + P_c}. \tag{10}$$

Here, we aim at maximizing the EEE with EC, delay and power constraints. Thus, the optimization problem is formulated as

$$\begin{aligned} \max_{\rho\geq 0,\theta\geq 0}\ & EEE, \\ s.t\ \ & EC(\rho,\theta) \geq \mu, \\ & P_{nb}e^{-\theta\mu D_{max}} \leq P_{out\_delay}, \\ & \rho \leq P_{max}. \end{aligned} \tag{11}$$

The optimal value of θ can be obtained from the second constraint as

$$\theta^*(\rho) = \frac{1}{\mu D_{max}}\log\frac{\mu}{P_{out}E_z\left[C\right]} \tag{12}$$

For $\theta \geq 0$ we should have $E_z\left[C\right] \leq \frac{\mu}{P_{out}}$ Substituting for θ^* in (12), we formulate the problem as

$$\begin{aligned} \max_{p\geq 0} \ & \frac{\frac{-1}{\theta^*}\log E_z\left[\log(1+\rho z)^{-\theta^*}\right]}{\frac{\mu}{E_z[\log(1+\rho z)]}\zeta p + P_c}, \\ s.t \ & EC(p,\theta^*) \geq \mu, \\ & E_z\left[C\right] \leq \frac{\mu}{P_{out}}, \\ & \rho \leq P_{max}. \end{aligned} \tag{13}$$

In Fig. 2.4, we plot the maximum EEE in (13) considering both the case of always full buffer and empty buffer probability for $\mu = 2$, $\rho = 30dB$, $\zeta = 2.5$ and $P_c = 10$. For the full buffer, we set $P_{nb} = 1$ in (12) resulting in

$$\theta^*(\rho) = \frac{1}{\mu D_{max}} \log \frac{1}{P_{out}}. \tag{14}$$

The results shows that considering empty buffer probability maximizes the EEE over the case of always full buffer. Extending the delay limit and relaxing delay outage probability (i.e allowing a higher delay outage probability) enhances the EEE as well.

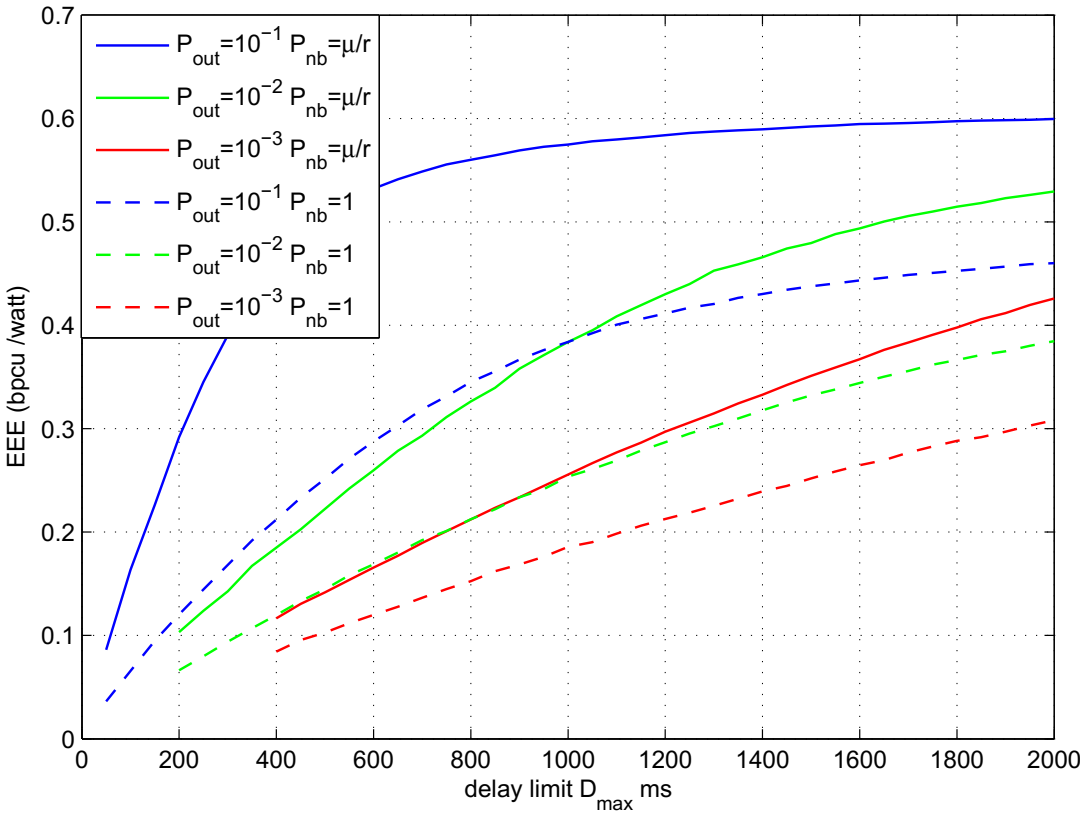

Figure 2.4. Comparison between EEE maximization in case of empty buffer probability and always full buffer for $\mu = 2$, $\rho = 30dB$, $\zeta = 2.5$ and $P_c = 10$. and different delay outage probabilities P_{out_delay}.

Fig. 2.5 shows a plot for the EEE resulting from EEE maximization and EC maximization for different values of maximum transmission power P_{max} where the maximum delay is fixed at $D_{max} = 400$, $P_{out\_delay} = 10^{-1}$ and the rest of parameters are the same as in the previous figure. We also consider both cases of empty buffer probability and always full buffer. The figure shows that EEE maximization results in higher EEE rather than maximizing the EC. Furthermore, accounting for empty buffer probability increases the EEE compared to the case when the buffer is always full.

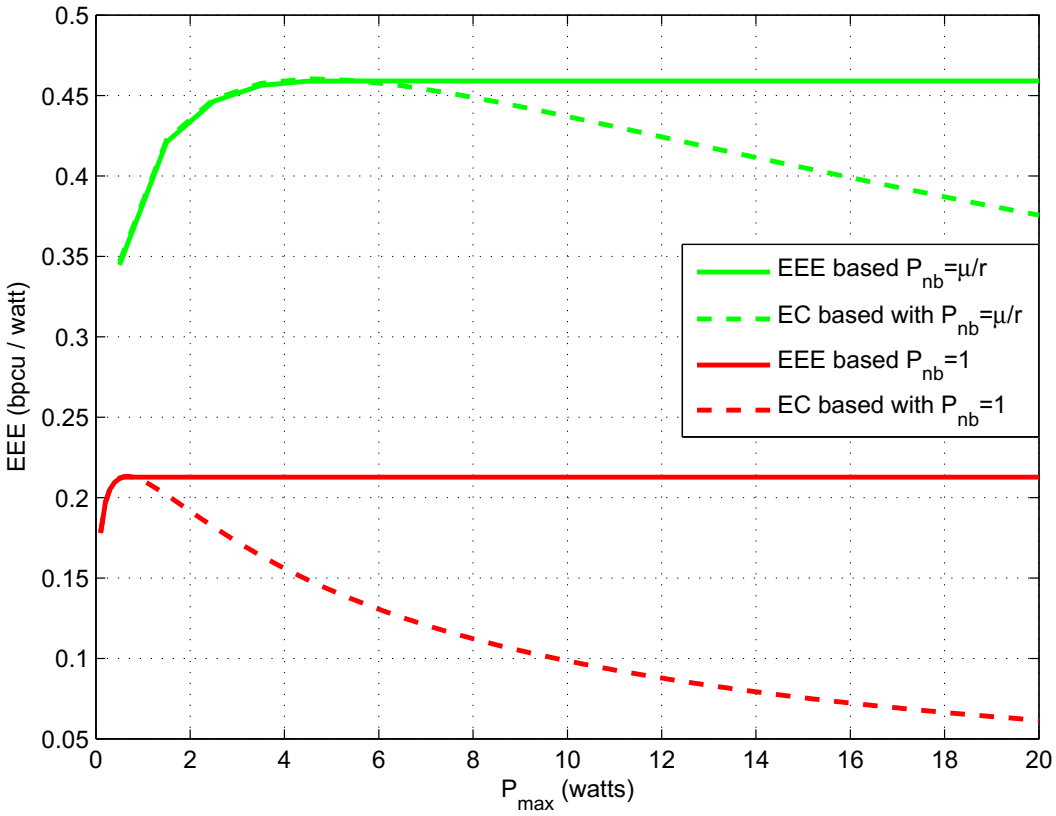

Figure 2.5. Comparison between the effect of EEE and EC maximization on the EEE for different values of maximum transmit power P_{max} in cases of empty buffer probability and always full buffer for $\mu = 2$, $\zeta = 2.5$, $P_c = 10$, $P_{out\_delay} = 10^{-1}$ and $D_{max} = 400$.

3. EFFECTIVE CAPACITY OF MULTI-USER NETWORKS IN THE FINITE BLOCKLENGTH REGIME

In this chapter, we obtain a closed form approximation for the per-user effective capacity in a multi-user network operating in the finite blocklength regime and we characterize the optimum error probability for the EC maximization for all cases. The general Nakagami-m model is first considered then we study Rayleigh fading as a special case.

3.1. System layout

We consider a transmission scenario in which N users (or users) transmit packets with equal power to a common controller through a block fading interference channel with blocklength T_f as shown in Figure 3.1. Given that all users transmit at the same time slot, the controller tries to decode the transmitted symbols arriving from all of them. When the controller decodes user's data, the other users appear as interference to it. For this model, imagine that a user needs to raise its EC temporarily for a critical reason. Later on, we study the interference alleviation scenarios for one user at a certain time slot while all users also keep transmitting at the same time. The channel fading coefficient $|h|^2$ is assumed to be constant for each block of T_f symbol periods and changes from one block to another. The received vector $\mathbf{y}_n \in \mathbb{C}^n$ of user n is given by

$$\mathbf{y}_n = h_n \mathbf{x}_n + \sum_{s \neq n} h_s \mathbf{x}_s + \mathbf{w} \tag{15}$$

where $\mathbf{x}_n \in \mathbb{C}^n$ is the transmitted packet of user n, h_n is the fading coefficient for user n; the index s includes all $N-1$ interferes which collide with user n, and $\mathbf{w}$ is the additive complex Gaussian noise vector whose entries are circularly symmetric and assumed to have a unit variance. Given the signal to noise ratio ρ of a single user, the signal-to-interference-plus-noise ratio (SINR) of any user n is

$$\rho_i = \frac{\rho}{1 + \rho \sum_s |h_s|^2}. \tag{16}$$

To simplify the analysis, we assume that: *i*) each user always has a packet to transmit (buffer is always non-empty); *ii*) all users are equidistant from the common controller (i.e., same path loss); and *iii*) the fading coefficients h_s are independent and identically distributed and perfectly known to the receiver. Thus, the interference resulting from users in set s can be modeled as additive Gaussian noise as in [19] [38], then (16) reduces to

$$\rho_i = \frac{\rho}{1 + \rho\,(N-1)}. \tag{17}$$

The channel is assumed to be Nakagami-m block fading where the fading coefficients remain constant over T_f symbols which spans the whole packet duration. For

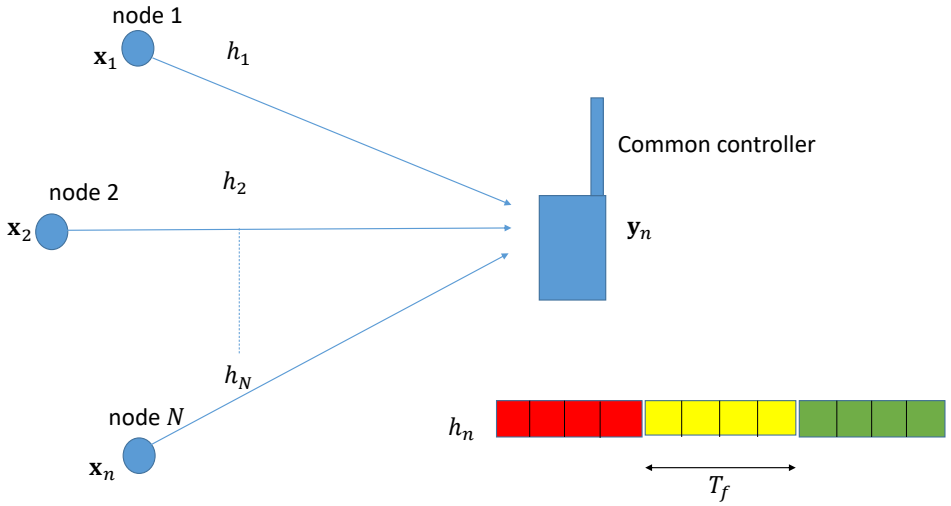

Figure 3.1. System layout where N users communicate to a common controller in a block-fading scenario.

Nakagami-m channels, the fading coefficients $z = |h|^2$ have the following probability density function distribution [31]

$$f_z(z) = \frac{m^m z^{m-1}}{\Gamma(m)} e^{-mz}, \tag{18}$$

where low values of m mark severe fading, high values of m mark the presence of line of sight (LOS) and $m = 1$ represents Rayleigh fading.

For this model, the normalized achievable rate in bits per channel use (bpcu) is given by

$$r_i = \log_2(1 + \rho_i z) - \sqrt{\frac{1}{T_f}\left(1 - \frac{1}{(1+\rho_i z)^2}\right)} Q^{-1}(\epsilon) \log_2(e), \tag{19}$$

where ρ_i is the signal-to-interference-plus-noise ratio (SINR). Leveraging the effect of interference via (6) , the per-user EC for this model would be

$$EC(\rho_i, \theta, \epsilon) = -\frac{1}{T_f \theta} \log\left(E_{z=|h|^2}\left[\epsilon + (1-\epsilon)e^{-T_f \theta r_i}\right]\right), \tag{20}$$

which is considered to be concave in ϵ as the only changed term of the equation is the SINR. Assuming always full buffer, the per-user EEE is given by

$$EEE = \frac{-\frac{1}{T_f\theta} \log\left(E_{z=|h|^2}\left[\epsilon + (1-\epsilon)e^{-T_f \theta r_i}\right]\right)}{\zeta\rho + P_c}. \tag{21}$$

For constant transmit power and always full buffer, the per-user EEE is concave in ϵ and there is a unique maximizer in ϵ for both EC and EEE which is obtained later in Lemma 1. This is because the denominator of (21) does not depend on ϵ; so maximization of EC consequently maximizes the EEE.

3.2. Per-node effective capacity in the finite blocklength regime

In what follows, we shall represent the EC expression for Nakagami-m channels; then we proceed with Rayleigh fading as a special case in our analysis.

Lemma 1. *The per-user effective capacity for a network of N users communicating in a Nakagami-m block fading collision channel with blocklength T_f is approximated by*

$$\begin{aligned} EC(\rho_i,\theta,\epsilon) \approx -\frac{1}{T_f\theta}\frac{m^m}{\Gamma(m)}\log\Bigg[\epsilon\,\frac{\Gamma(m)}{m^m} \\ +(1-\epsilon)\int_0^\infty (1+\rho_i z)^d \sum_{n=0}^{2}\frac{(cx)^n}{n!} z^{m-1}e^{-mz}dz\Bigg]. \end{aligned} \tag{22}$$

Proof. Using (18) in (6), we attain

$$EC(\rho_i,\theta,\epsilon) = -\frac{1}{T_f\theta}\frac{m^m}{\Gamma(m)}\log\left(\int_0^\infty \left(\epsilon+(1-\epsilon)e^{-\theta T_f r_i}\right) z^{m-1}e^{-mz}dz\right), \tag{23}$$

$$e^{-\theta T_f r_i} = e^{-\theta T_f \log_2(1+\rho_i z)}.e^{\theta\sqrt{T_f(1-\frac{1}{(1+\rho_i z)^2})}Q^{-1}(\epsilon)\log_2 e}. \tag{24}$$

Analyzing,

$$\begin{aligned} e^{-\theta T_f \log_2(1+\rho_i z)} &= e^{\frac{-\theta T_f \log(1+\rho_i z)}{\log 2}} \\ &= (1+\rho_i z)^{\frac{-\theta T_f}{\log 2}} \\ &= (1+\rho_i z)^d. \end{aligned} \tag{25}$$

where $d = \frac{-\theta T_f}{\log(2)}$. Also let $c = \theta\sqrt{T_f}Q^{-1}(\epsilon)\log_2 e$ and $x = \sqrt{(1-\frac{1}{(1+\rho_i z)^2})}$; then we have

$$e^{\theta\sqrt{T_f(1-\frac{1}{(1+\rho_i z)^2})}Q^{-1}(\epsilon)\log_2 e} = e^{cx}, \tag{26}$$

where $e^{cx} = \sum_{n=0}^{\infty}\frac{(cx)^n}{n!}$. It follows from (24),(25) and (26) that the expression in (23) can be written as

$$\begin{aligned} EC(\rho_i,\theta,\epsilon) = -\frac{1}{T_f\theta}\frac{m^m}{\Gamma(m)}\log\Bigg[\int_0^\infty \epsilon\, z^{m-1}e^{-mz}dz \\ +(1-\epsilon)\int_0^\infty (1+\rho_i z)^d \sum_{n=0}^{\infty}\frac{(cx)^n}{n!} z^{m-1}e^{-mz}dz\Bigg]. \end{aligned} \tag{27}$$

The infinite series in (27) can be truncated to a finite sum of terms and we evaluate the accuracy of the expression noting that the accuracy increases with the number of terms. But, it is noticed that when testing for different system parameters (N, ρ, θ, T_f), the accuracy for expanding 1 term is 92.7%, 2 terms is 99% and 99.9% for 3 terms only. This is depicted in Figure 3.2 when comparing to the expectation plot resultant from 10^7 monte-carlo runs for the parameters $N = 1, \rho = 2, T_f = 1000$, and $\theta = 0.01$, in a Rayleigh fading channel ($m = 1$). Henceforth, in our analysis, 3 terms will be enough and (27) reduces to (22). □

Corollary 1. *There is a unique maximizer in ϵ for the per-user EC in general Nakagami-m block fading collision channels which is given by*

$$\epsilon^*(\rho_i, c, d) \approx \arg\min\ \epsilon\ \frac{\Gamma(m)}{m^m} + (1-\epsilon)\int_0^\infty (1+\rho_i z)^d \sum_{n=0}^{2} \frac{(cx)^n}{n!} z^{m-1} e^{-mz} dz. \tag{28}$$

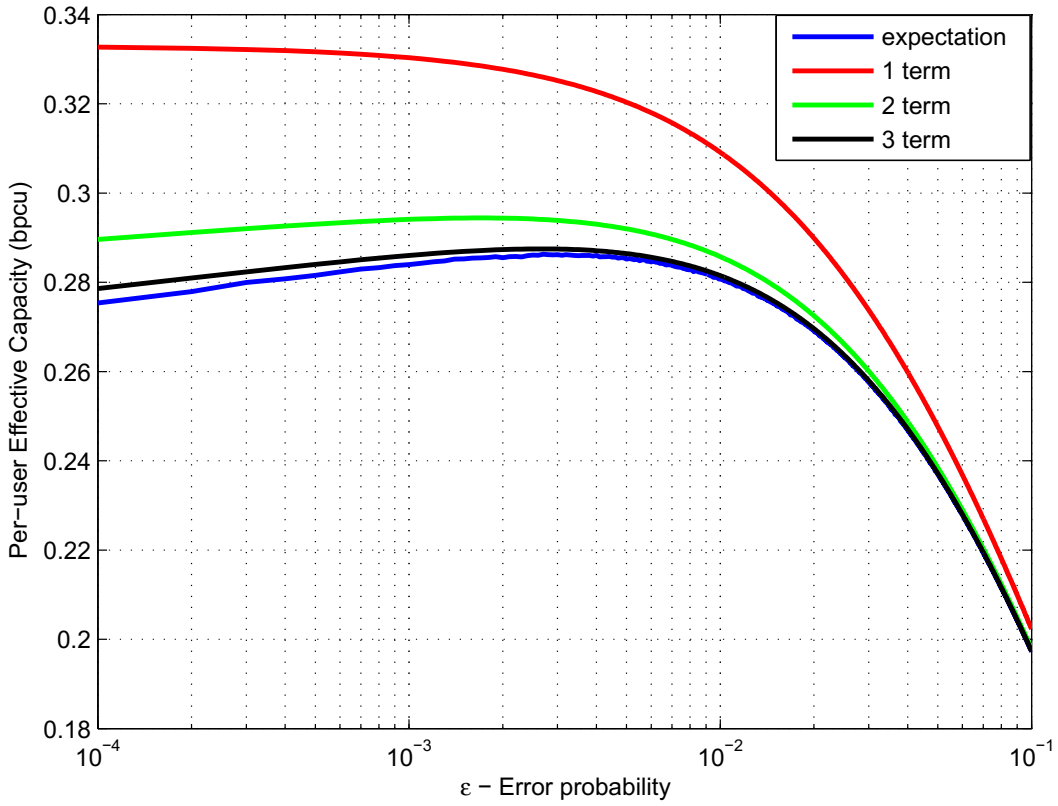

Figure 3.2. EC as a function of error outage probability ϵ for different number of users, with $T_f = 1000, \rho = 2$, and $\theta = 0.01$.

Proof. The expectation in (6) is shown to be convex in ϵ in [23] independent of the distribution of channel coefficients $z = |h|^2$. Thus, it has a unique minimizer ϵ^* which is consequently the EC maximizer given by (28) □

Note that c is not a function of z, so it can be taken out of the integration which simplifies the optimization problem. To obtain the maximum per-user effective capacity EC_{max}, we simply insert ϵ^* into (22).

Corollary 2. *The per-user effective capacity for a network of N users communicating in a Rayleigh block fading collision channel with blocklength T_f is approximated as*

$$EC_{Ry}(\rho_i, \theta, \epsilon) \approx -\frac{1}{T_f\theta}\log\left[\epsilon + (1-\epsilon) * \int_0^\infty (1+\rho_i z)^d \sum_{n=0}^{2} \frac{(cx)^n}{n!} e^{-z} dz\right]. \quad (29)$$

and the corresponding optimum probability of error is given by

$$\epsilon^*(\rho_i, c, d) \approx \arg\min \epsilon + (1-\epsilon) \int_0^\infty (1+\rho_i z)^d \sum_{n=0}^{2} \frac{(cx)^n}{n!} e^{-z} dz. \quad (30)$$

Proof. The proof is straight forward when substituting for $m = 1$ in (22). □

For fixed rate transmission, and approximation for the optimum value of r_f^* that maximizes the EC can be obtained analytically from (proof is straight forward)

$$r_f^* \approx arg\,max\;\; EC(\rho_i, \theta, r_f) = -\frac{\log\left(\frac{\epsilon^* + (1-\epsilon^*)\int_0^\infty (1+\rho_i z)^d \sum_{n=0}^{2} \frac{(cx)^n}{n!} e^{-z} dz - \epsilon^*}{1-\epsilon^*}\right)}{\theta T_f}. \quad (31)$$

Now that we obtained a non-statistical solution for EC, we proceed with studying the effect of multi-user interference and various fading scenarios on the per-user EC. In Figure 3.3, we examine the effect of different types of fading by plotting the per-user EC vs the probability of error ϵ for different values of fading parameter m using Lemma 1 where the network parameters are set as $T_f = 500$, $\rho = 2$, and $\theta = 0.01$. The figure shows that for a 2 users network, the per-user EC in Ricean fading ($m = 1.2$) is higher than Rayleigh case ($m = 1$) while it is the lowest in case of severe fading ($m = 0.8$). This is because as the value of the parameter m increases, the LoS transmitted component of the signal increases and consequently the signal strength at the receiver which boosts the EC according to [39].

Figure 3.4 addresses the effect of interference on the per-user EC when several users transmit to a common controller at the same time in a Rayleigh block fading channel with blocklength $T_f = 500$ where $\rho = 2$, and $\theta = 0.01$. It is clear that the per-user EC decreases when increasing N as more interference is added to the system. Notice that the EC curves are concave in ϵ and hence, have a unique maximizer which is obtained from (28). Another observation worth mentioning is that the optimum probability of error ϵ^* which maximizes the EC becomes higher when increasing the number of users. From now on, our analysis and results will focus on the Rayleigh fading case where the same procedures can be applied for any type of channels simply by changing the value of m.

The previous 2 figures highlight the trade off between per-user EC and error probability ϵ. It is apparent that we can get lower ϵ by sacrificing only a small amount of EC. For example, Figure 3.4 shows that for the 2 users network, if we tolerate a decrease in the EC from 0.192 to 0.186 bpcu, the error probability ϵ improves to 10^{-3} instead of 8×10^{-3}. This means that sacrificing a 3% of the EC maximum value boosts the error probability by nearly 800% and hence, leads to a dramatic enhancement of reliability. In a future work, we are planning to analyze the EC-ϵ throughly with a target of maximizing the transmission error reliability with some EC constraints reflecting the delay issues.

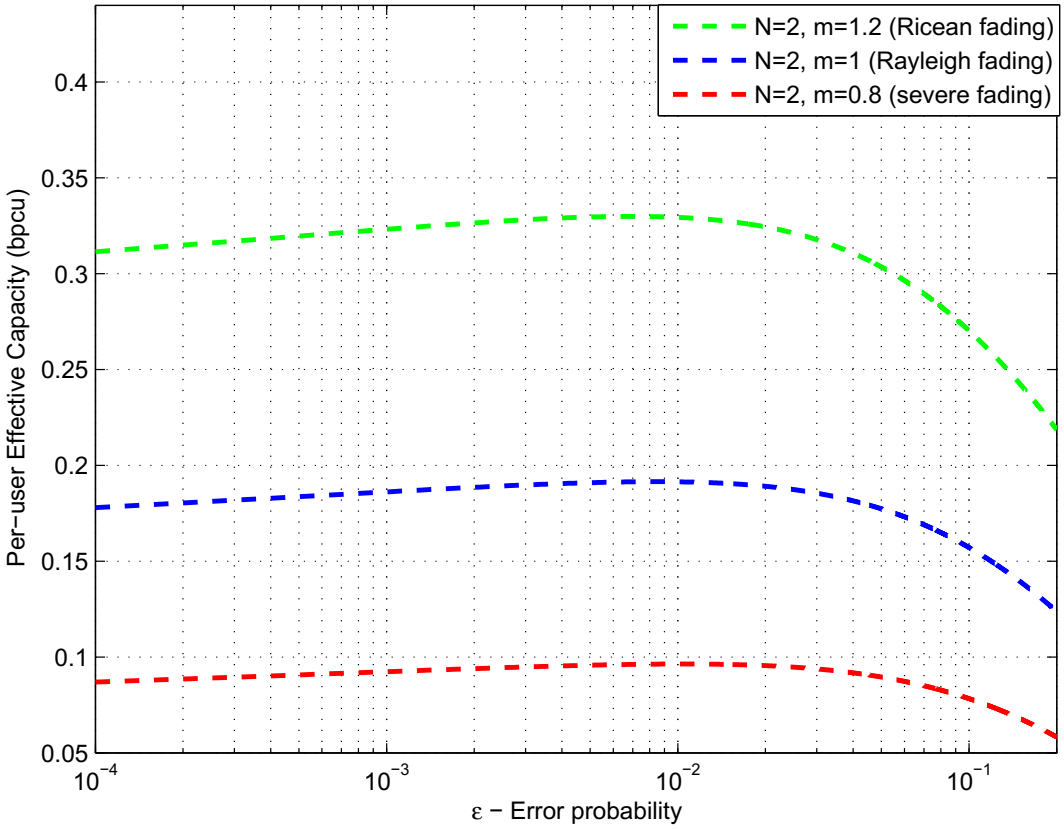

Figure 3.3. EC as a function of error outage probability ϵ for $N = 2$ users, with $T_f = 500, \rho = 2$, and $\theta = 0.01$.

3.3. Maximization of effective capacity in the ultra-reliable region

In this section, we discuss the EC maximization in ultra reliable (UR) region. We maximize the EC so that the error outage probability stays below a very small target value ϵ_t. We define the optimization problem as

$$\max_{\epsilon \leq \epsilon_t} EC_{Ry}(\rho_i, \theta, \epsilon) \approx -\frac{1}{T_f \theta} \log \left[\epsilon + (1-\epsilon) * \int_0^\infty (1+\rho_i z)^d \sum_{n=0}^{2} \frac{(cx)^n}{n!} e^{-z} dz \right]. \tag{32}$$

which can be interpreted to

$$\begin{aligned} &\min \psi(\epsilon) = \epsilon + (1-\epsilon) * \int_0^\infty (1+\rho_i z)^d \sum_{n=0}^{2} \frac{(cx)^n}{n!} e^{-z} dz, \\ &s.t \ \ \epsilon \leq \epsilon_t. \end{aligned} \tag{33}$$

Due to the convexity of $\psi(\epsilon)$, the first derivative of $\psi(\epsilon)$ is positive if ϵ is greater than the global maximum and vice versa. Thus, we can check if the optimum solution

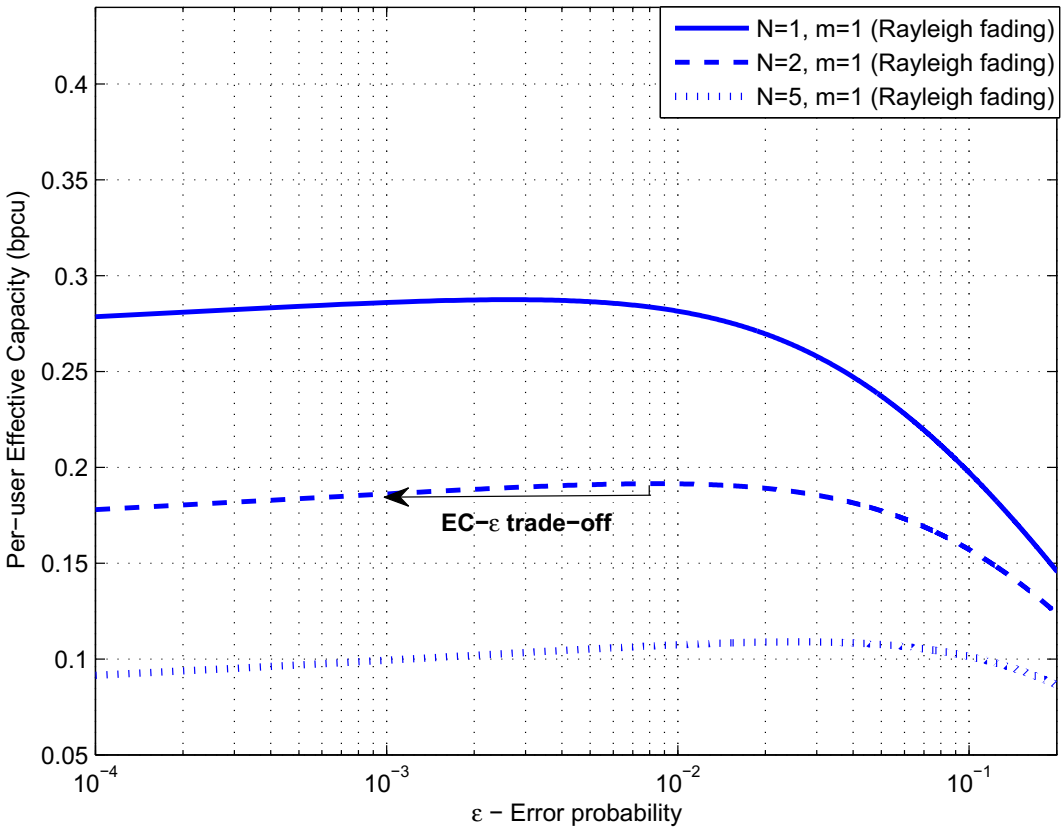

Figure 3.4. EC as a function of error outage probability ϵ for different number of users, with $T_f = 500$, $\rho = 2$, and $\theta = 0.01$.

is given by ϵ_t or not through the first derivative of $\psi(\epsilon)$. To elucidate, we write down the Lagrangian of (33) as

$$\mathfrak{L}(\epsilon, \lambda) = \psi(\epsilon) + \lambda(\epsilon - \epsilon_t), \tag{34}$$

and we have the following Karush−Kuhn−Tucker (KKT) conditions

$$\begin{aligned} \frac{\partial \psi(\epsilon)}{\partial \epsilon} + \lambda &= 0 \\ \lambda(\epsilon - \epsilon_t) &= 0. \end{aligned} \tag{35}$$

From the second condition, if λ is greater than zero, this means that the constraint is active and $\epsilon^* = \epsilon_t$ and $\frac{\partial \psi(\epsilon)}{\partial \epsilon}|_{\epsilon=\epsilon_t}$ is indeed negative. Reversing this conclusion, we can infer if the constraint is active or not from the sign of $\frac{\partial \psi(\epsilon)}{\partial \epsilon}|_{\epsilon=\epsilon_t}$ so that

$$\epsilon^* = \begin{cases} \epsilon_t & \frac{\partial \psi(\epsilon)}{\partial \epsilon}|_{\epsilon=\epsilon_t} < 0 \\ \arg\min_{\epsilon \geq 0} \ \epsilon + (1-\epsilon) \int_0^\infty (1+\rho_i z)^d \sum_{n=0}^2 \frac{(cx)^n}{n!} e^{-z} dz, & \frac{\partial \psi(\epsilon)}{\partial \epsilon}|_{\epsilon=\epsilon_t} > 0 \end{cases}. \tag{36}$$

The first derivative of $\psi(\epsilon)$ with respect to ϵ can be derived to be

$$\frac{\partial \psi(\epsilon)}{\partial \epsilon} = 1 - (1-\epsilon)\delta\sqrt{2\pi}e^{\frac{(Q^{-1}(\epsilon))^2}{2}}(I_2 + \delta I_3) - I, \tag{37}$$

where

$$\begin{aligned}
I_2 &= \int_0^\infty (1+\rho_i z)^d \sqrt{1 - \frac{1}{(1+\rho_i z)^2}} e^{-z} dz, \\
I3 &= \int_0^\infty (1+\rho_i z)^d \left(1 - \frac{1}{(1+\rho_i z)^2}\right) e^{-z} dz, \\
I &= \int_0^\infty (1+\rho_i z)^d \left(1 + c\sqrt{1 - \frac{1}{(1+\rho_i z)^2}} + \frac{c^2}{2}\left(1 - \frac{1}{(1+\rho_i z)^2}\right)\right) e^{-z} dz, \\
\delta &= \theta\sqrt{T_f}\log_2 e.
\end{aligned} \tag{38}$$

4. MULTI-USER INTERFERENCE ANALYSIS AND COMPENSATION

In the previous chapter, we have clarified how the existence of multiple users affects the per-user EC degrading it. It has been shown that as networks become denser, the per-user EC significantly declines due to increases interference. In future technologies such as vehicular networks, it is essential to maintain reasonable data rates with strict delay constraints even if there are lots of vehicles operating in urban areas and the network becomes denser. There are plenty of methods to manage interference such as scheduling algorithms. However, we get to suppose that all users transmit at the same time and define methods to alleviate interference when a certain user requires its EC to be restored at least temporarily.

In this chapter, we study the trade-off between EC, transmit power ρ, and delay constraint θ in multi-user networks lightly dense and heavily dense networks. We propose 3 procedures to restore the EC for one user which are power control, relaxation of delay constraint and joint compensations which combines the first two methods. We study the trade-off between the power and delay and characterize the optimum percentage of compensation that should be performed by each method in the joint compensation.

4.1. Interference cancellation via power control

The method of power control depends on increasing the SNR of a certain user n to allow it recover from the interference effect. In this section, we determine the amount of extra power needed by this user in order to compensate for the decrease in EC when many users are present and interference increases. After that, we study the behavior of this method when varying the network parameters (ρ, θ, N). First, let ρ_c be the new SNR of user n (the other users still transmit with SNR equal to ρ). Then we simply equate the SINR equation in (17) to the case where no collision occurs ($N = 1$). That is

$$\begin{aligned} \frac{\rho_c}{1+\rho(N-1)} &= \rho \\ \rho_c &= \rho\,(1+\rho(N-1)). \end{aligned} \tag{39}$$

When a certain user transmits with SNR of ρ_c, its EC is the same as in the case when transmitting with SNR equals to ρ while other users are silent. As an example, consider 3 colliding users where $T_f = 500, \theta = 0.01$, and $\rho = 0.5$. Applying (39), we get $\rho_c = 1$. Hence, the interference effect is canceled for a certain user by boosting its SNR from 0.5 to 1. Notice that the amount of increase in SNR of the compensating user does not depend on the blocklength T_f, delay exponent θ, it only depends on the number of users N in a direct proportional relation. This is because the amount of power needed to compensate one user increases when increasing the number of users N where more interference is added to the system as depicted in the previous chapter.

The method of power control is simple. Nevertheless, its drawback lies in the effect of extra interference affecting other users due to the power increase of the recovering user. To elucidate more, Figure 4.1 shows the effect of collision of 5 users before and

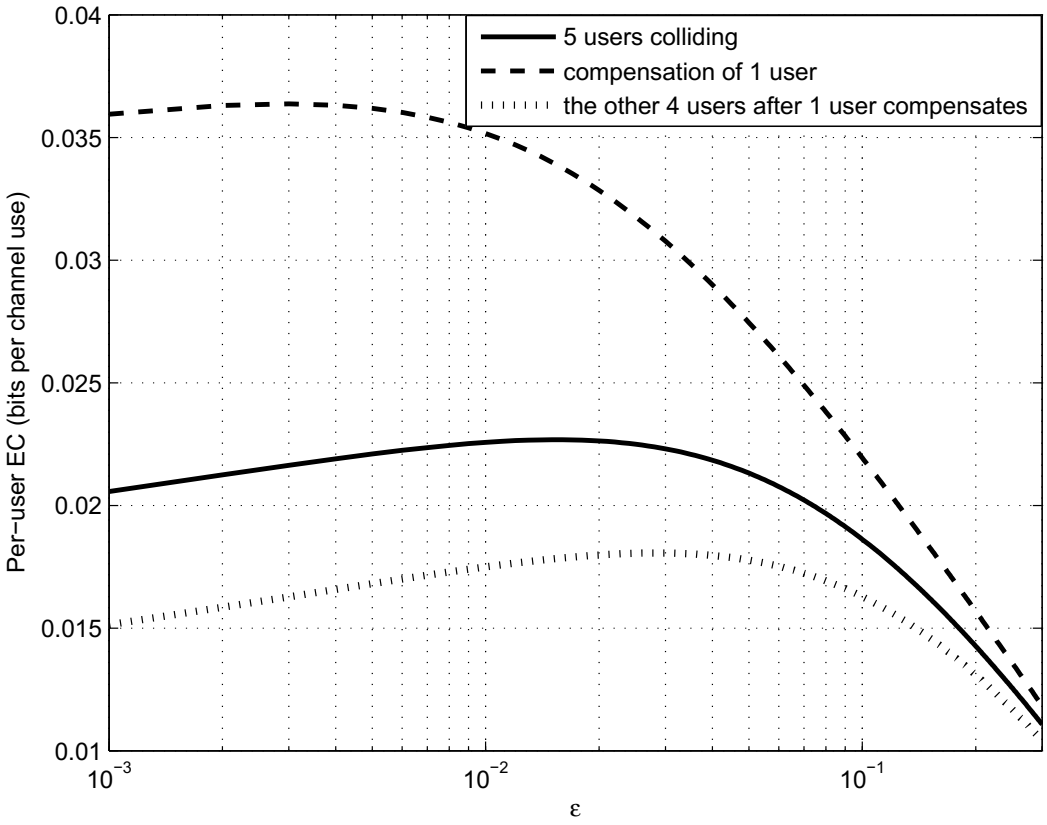

Figure 4.1. Effect of compensation of 1 user via power control as a function of error outage probability ϵ with $T_f = 1000, \theta = 0.1$, and $\rho = 1$.

after compensation of one user via power control for a network with the parameters $T_f = 1000, \theta = 0.1$, and $\rho = 1$. We plot the per-user EC before compensation of 1 user; and then we compare it to the effective capacities of the 4 remaining users after this one user compensates using (39). The figure shows that the EC of the compensating user rises to its original level as if it is not affected by interference while the per-user EC of the other users falls down due to the extra interference caused by rising the SNR of the compensating user.

From (39), we define the SINR of other users colliding in the same system (users in set s) after the compensation of 1 user as

$$\rho_s = \frac{\rho}{1 + \rho_c + \rho(N-2)} \tag{40}$$

$$= \frac{\rho}{1 + \rho\,(\rho+1)(N-1)}. \tag{41}$$

Now, we are interested in comparing the per-user EC in 3 cases: *i*) No collision, *ii*) collision without compensation, and *iii*) collision with compensation of 1 user. Here, we look for the maximum achievable per-user EC in each case. Define the collision loss factor α as the ratio between the maximum per-user effective capacity EC_{max} of

the users in the network in case of collision and in case of no collision (i.e, every user is standing alone) as

$$\alpha = \frac{EC_{Ry}(\rho_i, \theta, \epsilon_i^*)}{EC_{Ry}(\rho, \theta, \epsilon^*)}, \tag{42}$$

where ϵ^* is the optimal error probability for the case of no collision ($N = 1$) and ϵ_i^* is the optimal error probability for the case of collision without compensation where both are obtained from (30). Collision loss factor α indicates the effect of collision on all users in the system without any user increasing its transmission power for compensation. To determine the effect of compensation of 1 user on the other users, we define the compensation loss factor α_c as the ratio between maximum EC of other users (set s) in case of 1 user compensation and in case of no compensation. That is

$$\alpha_c = \frac{EC_{Ry}(\rho_s, \theta, \epsilon_s^*)}{EC_{Ry}(\rho_i, \theta, \epsilon_i^*)}, \tag{43}$$

where ϵ_s^* is the optimum probability of error obtained from (28) when we set the SINR to ρ_s.

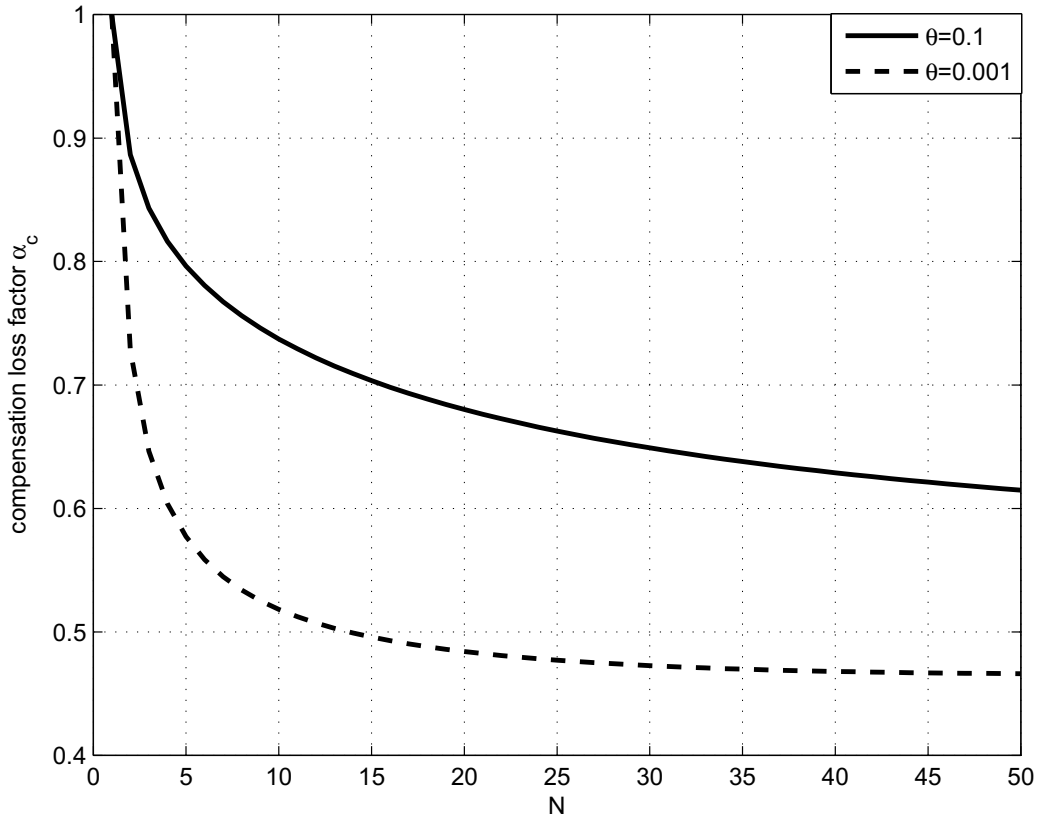

Figure 4.2. compensation loss factor α_c vs number of users N for a network operating in a Rayleigh block fading channel with blocklength $T_f = 1000$ and SNR $\rho = 1$.

Furthermore, we include the compensation factor γ_c as the ratio of the maximum achievable EC of the compensated user after and before compensation which is expressed as

$$\gamma_c = \frac{EC_{Ry}(\rho, \theta, \epsilon^*)}{EC_{Ry}(\rho_i, \theta, \epsilon_i^*)} = \frac{1}{\alpha}, \tag{44}$$

where γ_c is a gain factor (i.e., $\gamma_c \geq 1$). Finally, we define the total loss factor α_t as the ratio between the maximum attainable effective capacity of colliding users in the system (set s) when a user compensates to the maximum attainable EC of these users if they were not colliding at all. That is

$$\alpha_t = \frac{\alpha_c}{\gamma_c} = \alpha.\alpha_c. \tag{45}$$

It is worth mentioning that the amount of loss increases (i.e worse situation) when the loss factor decreases.

Consider a multi-user network with the parameters $T_f = 1000$ and $\rho = 1$. For this network, we plot the above mentioned compensation and loss factors to observe their behavior for different values of delay constraint θ and study how they are affected by increasing the number of users N.

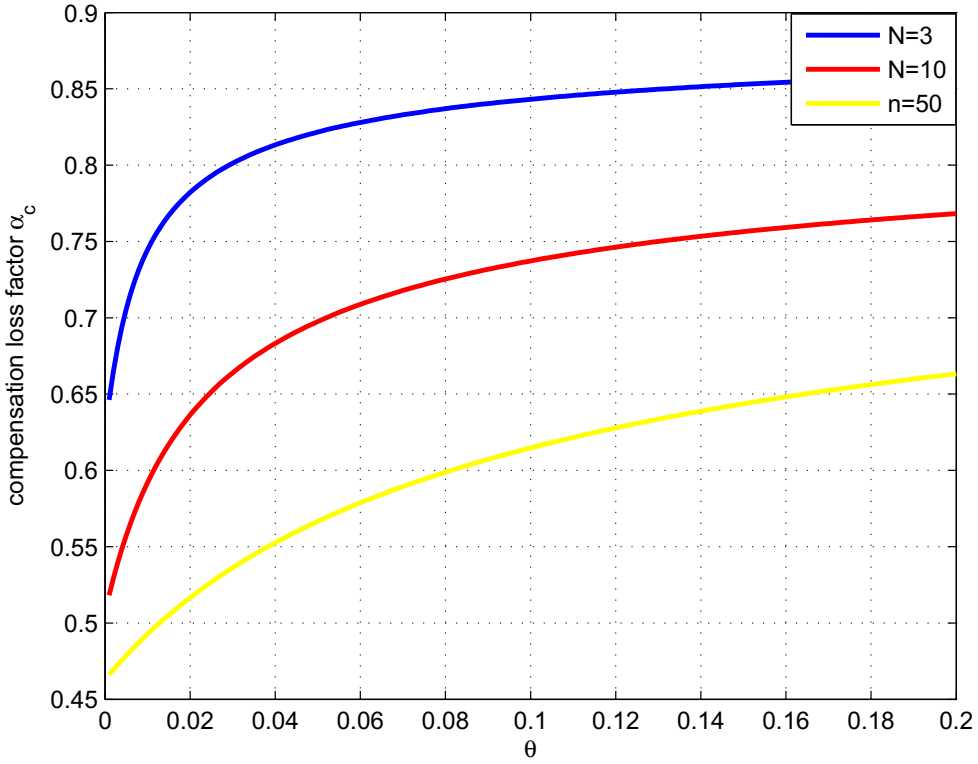

Figure 4.3. compensation loss factor α_c vs delay constraint θ for a network operating in a Rayleigh block fading channel with blocklength $T_f = 1000$ and SNR $\rho = 1$.

Figure 4.2 depicts the compensation loss factor α_c for different number of users N with $\theta = 0.1$ and 0.001. We notice that the compensation loss factor decreases rapidly

when the number of users N is less than 10. However, this attenuation becomes slower for higher number of users. In other words, the effect of compensating of 1 user on the other users tends to be constant as a function of the number of users when N is high. The figure also shows that the decrease of α_c is more rapid when the delay constraint is less stringent (lower values of θ); α_c decreases in a sharper way but then becomes more settled nearly around 5 for $N > 5$. The effect of compensation appears to be more severe for less stringent delay constraints.

In Figure 4.3, we plot the compensation loss factor α_c versus the delay constraint θ for different number of users N. The figure shows that the effect of compensation is more severe (i.e causing more degrading for the EC) for lower values of θ (less stringent delay constraint) which we concluded in the previous figure. This effect tends to be constant for $\theta > 0.1$ especially when we have a small number of users in the network. It is also apparent from the figure that the compensation loss factor lower (i.e higher loss) for higher number of users N. This is because the amount of power needed to compensate one user in a denser network is much higher which rises the interference level for other users

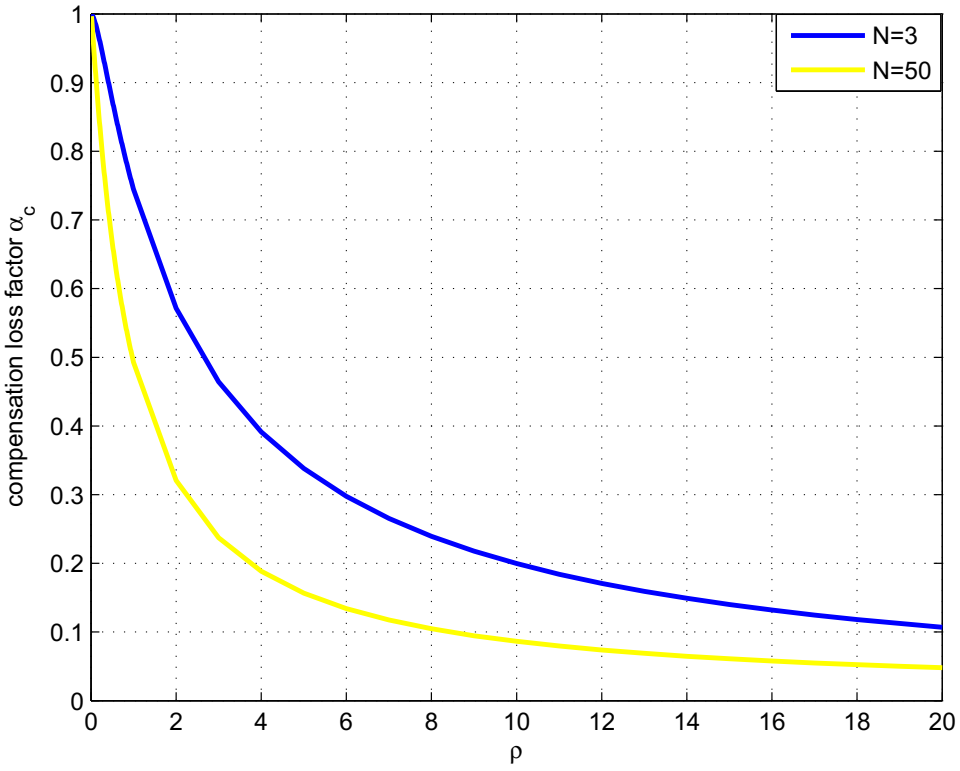

Figure 4.4. Compensation loss factor α_c vs SNR ρ for a network operating in a Rayleigh block fading channel with blocklength $T_f = 1000$, and delay constraint $\theta = 0.01$.

In Figure 4.4, we plot the compensation loss factor α_c, versus the SNR ρ for different number of users N. The figure shows that the effect of compensation 1 user on other users is more severe in high SNR regime as the value of compensation loss factor α_c

is lower. We also observe the effect of compensation on the other users is worse for denser networks which appears also from Figure 4.2 and Figure 4.3. To sum up, power controlled compensation is not feasible when dealing with dense networks, less strict delay bounds, or high SNR regime transmissions as its effect on other users in the network becomes more deleterious.

Figure 4.5 shows the compensation factor γ_c versus the number of users in the system N. γ_c appears to have a linear behavior as a function of N. That is, the effect of compensation for the compensated user increases linearly with N. The rate by which γ_c increases is faster for less θ. The compensation factor γ_c (compensation gain) is higher for less stringent delay constraint (less θ).

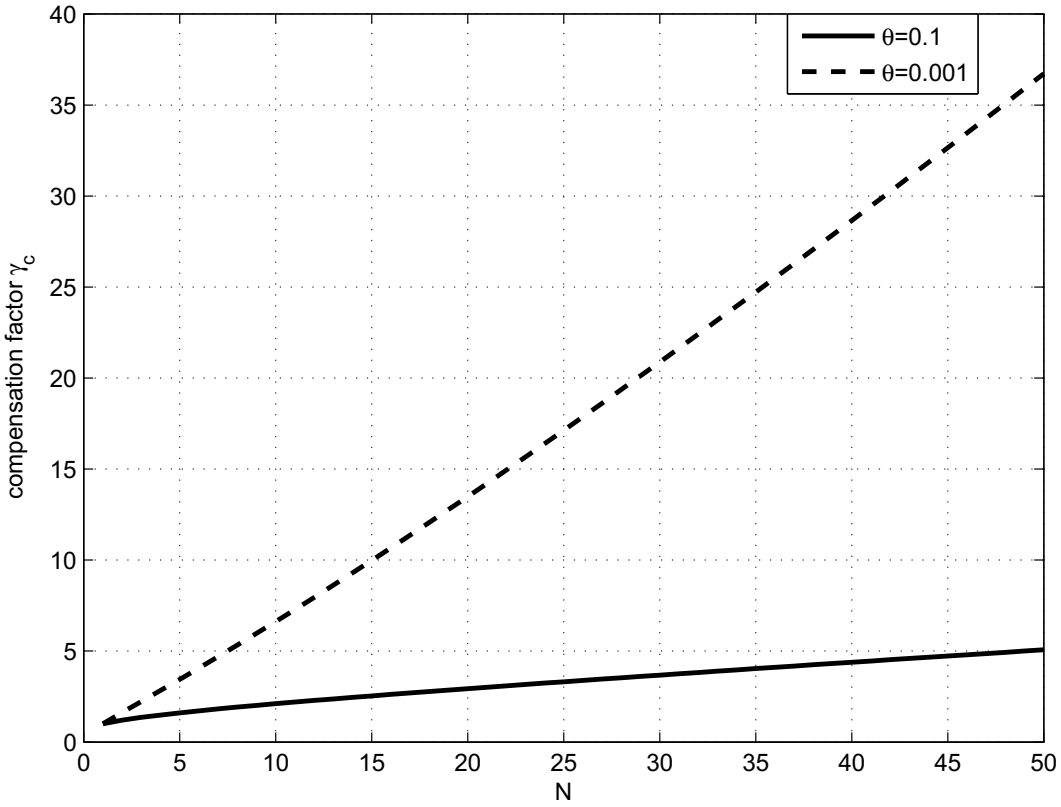

Figure 4.5. Compensation factor γ_c vs number of users N for a network operating in a Rayleigh block fading channel with blocklength $T_f = 1000$ and SNR $\rho = 1$.

Figure 4.6 depicts the compensation factor γ_c versus the delay constraint θ for different number of users. It is clear that compensation is more effective and powerful in case of less stringent delay constraint. It also appears that the compensation factor γ_c becomes higher when increasing the number of users. This is because the high interference in a highly dense network requires more compensation for a single user to restore its EC. We can also observe that the compensation factor γ_c is not much affected by the change of delay constraint θ for high values of θ (>0.1) reflecting more strict delay constraints.

Figure 4.7 depicts the compensation factor γ_c versus the transmission SNR ρ. While the compensation factor γ_c of less dense and highly dense networks is nearly the same

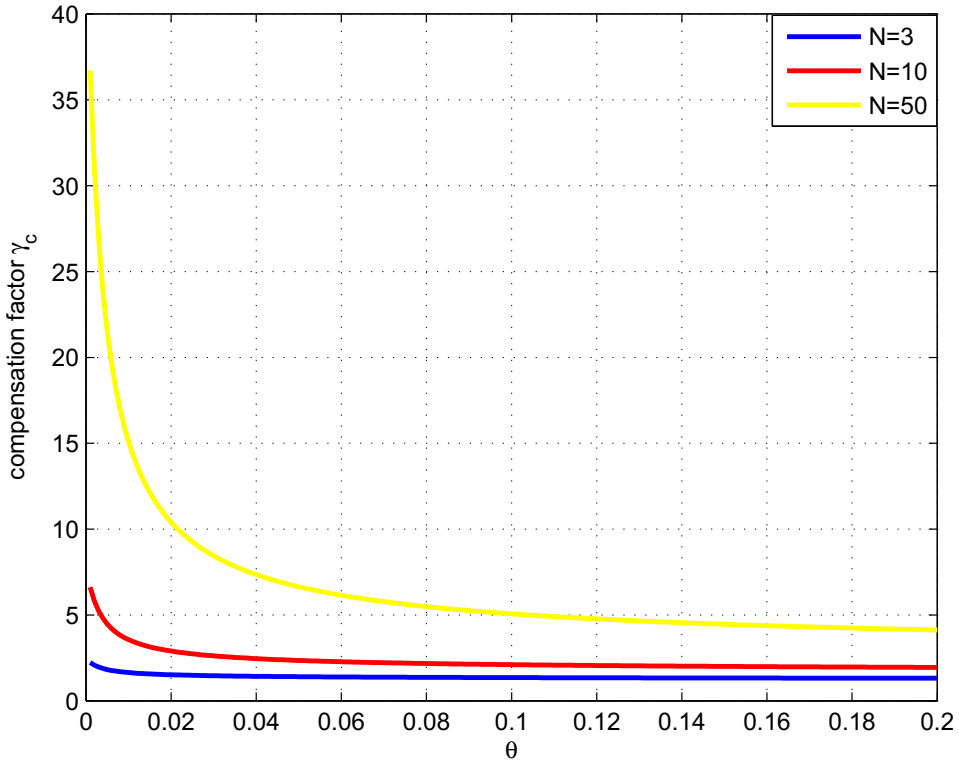

Figure 4.6. Compensation factor γ_c vs delay constraint θ for a network operating in a Rayleigh block fading channel with blocklength $T_f = 1000$ and SNR $\rho = 1$.

in the low SNR regime, compensation factor γ_c becomes significantly higher in highly dense networks than in networks with small number of users for the high SNR regime due to the same reason stated in the discussion of Figure 4.5 which is that highly dense network needs more compensation for a single user to restore its EC. It is clear that compensation is more effective and powerful in high SNR regime specially for networks with large number of users.

The collision loss factor α and the total loss factor α_t are plotted in Figure 4.8 versus the number users N. As observed from the figure, the total loss is nearly the same as the collision loss for small N. However, they have the same behavior as α_c where they appear to be settle at a certain value for $\theta > 0.1$. The gap between collision and total losses starts to appear and becomes almost constant for high number of users. This gap is tighter in case of small θ (i.e., the collision loss α is more dominant). Also, the loss factors (both collision and total) are lower in case of less stringent delay constraint θ. Both losses are more severe in case of less stringent delay constraint (lower θ). Thus, the effect of collision and compensation is more annoying in case of less stringent delay constraint (smaller θ). Furthermore, α and α_t has the same behavior as α_c which is shown in Figure 4.2. They decrease rapidly for small number of users and tend to be constant for high N.

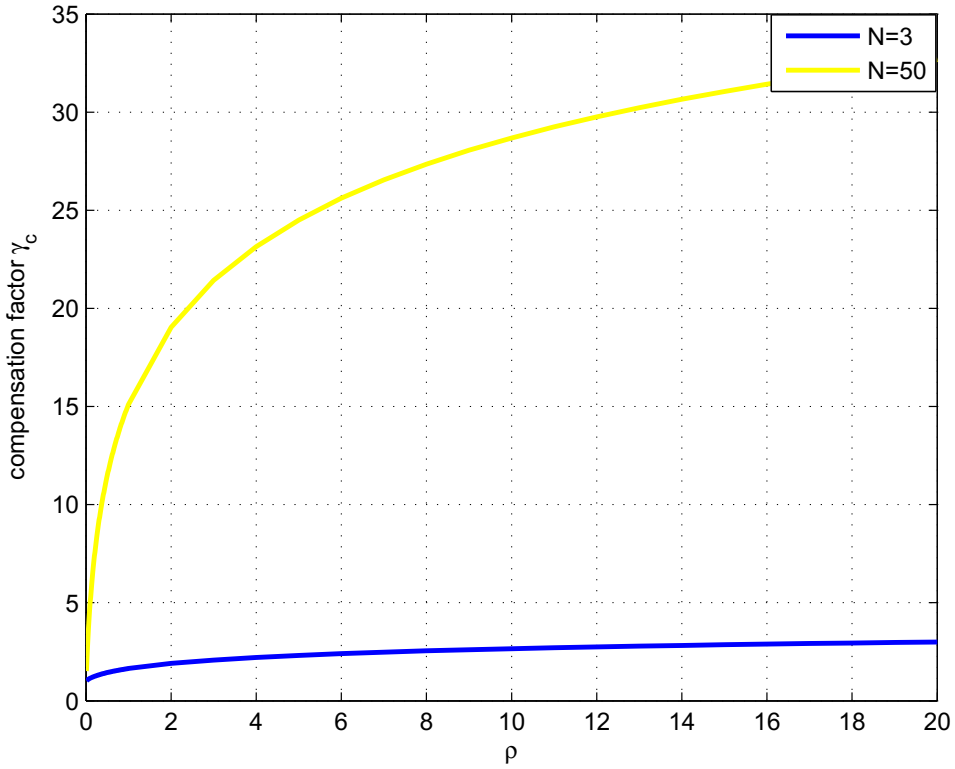

Figure 4.7. Compensation factor γ_c vs SNR ρ for a network operating in a Rayleigh block fading channel with blocklength $T_f = 1000$ and delay constraint $\theta = 0.01$.

We also plot the collision loss factor α and the total loss factor α_t are plotted for different number of users N in Figure 4.9 versus the delay constraint θ. The figure shows that both losses (collision and total loss) become higher as the delay constraint θ increases. Thus, the networks suffer more from interference and compensation via power control in case of tighter delay constraints. The loss factors (both collision and total) are lower for denser network mapping a higher loss. Although the gap between collision and total losses is tighter for high number of users (more dense networks), this gap remains nearly unaffected by the change of delay constraint θ.

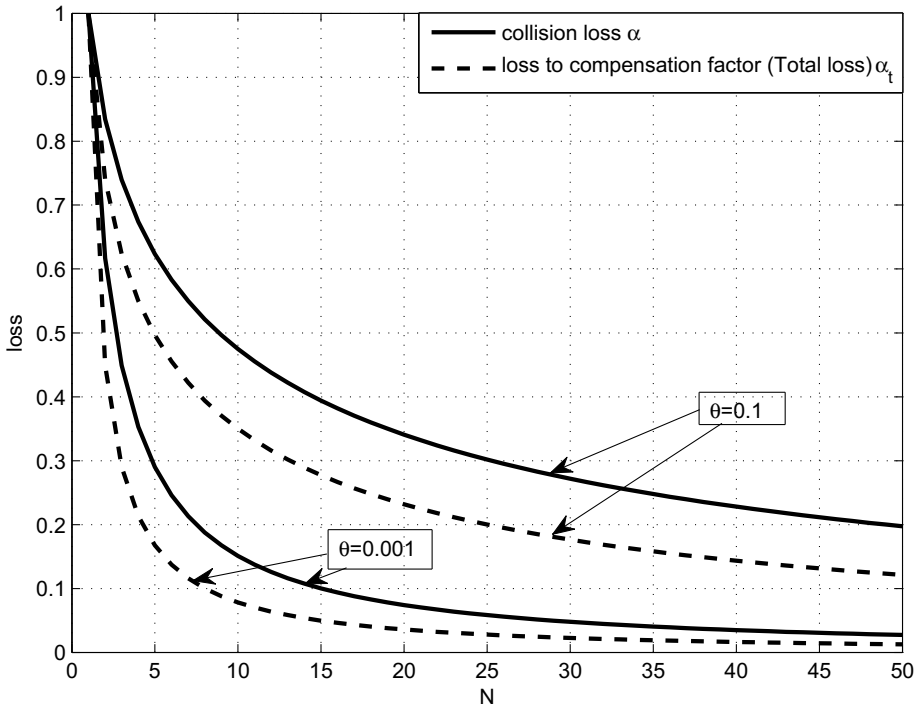

Figure 4.8. Loss factors α and α_t vs number of users N for a network operating in a Rayleigh block fading channel with blocklength $T_f = 1000$ and SNR $\rho = 1$.

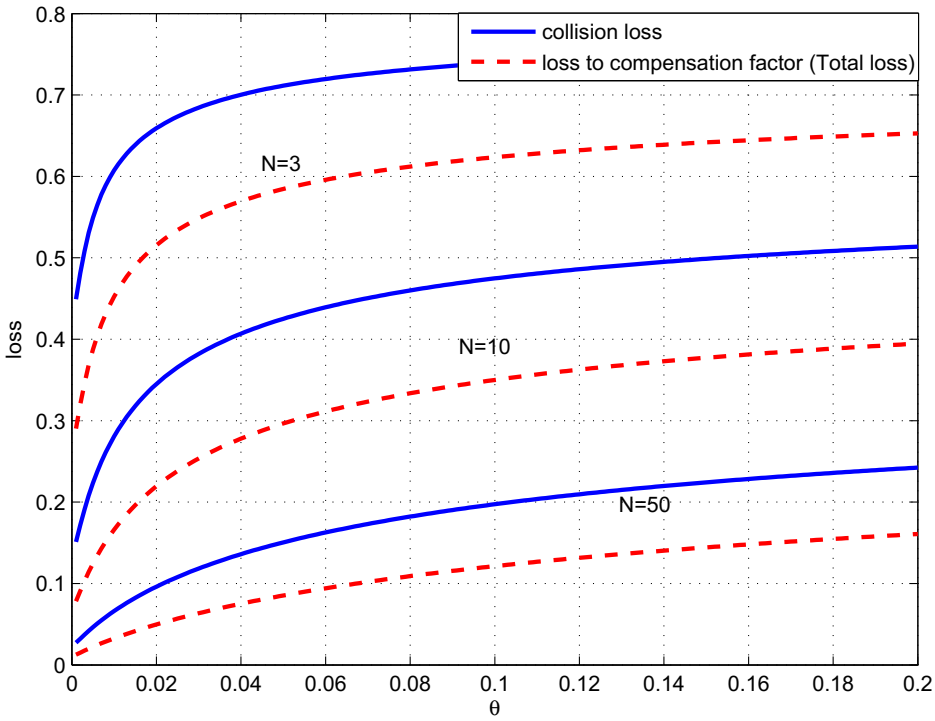

Figure 4.9. Loss factors α and α_t vs delay constraint θ for a network operating in a Rayleigh block fading channel with blocklength $T_f = 1000$ and SNR $\rho = 1$.

Finally, the collision loss factor α and the total loss factor α_t are also plotted in Figure 4.10 vs the SNR ρ for the delay exponent $\theta = 0.01$. The figure shows that collision loss factor α and the total loss factor α_t are more severe in High SNR Regime. It also appears that both as the number of users becomes higher, the loss factors becomes lower. Hence, denser networks suffer from higher losses as was discussed in Figure 4.9. The gap between these losses increases in the high SNR regime.

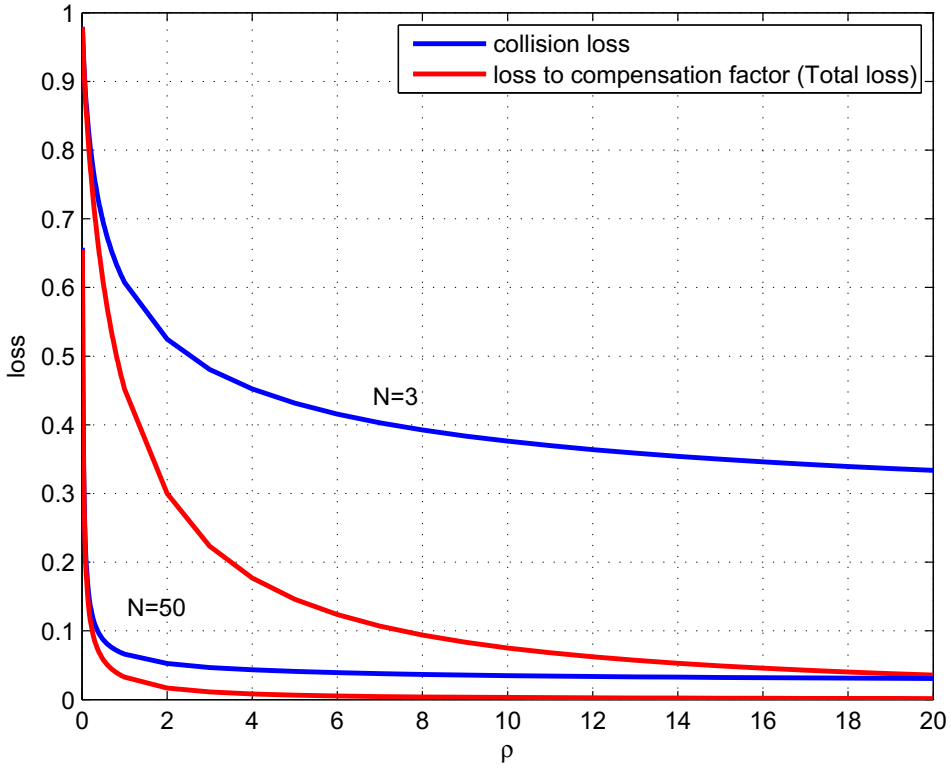

Figure 4.10. Loss factors α and α_t vs SNR ρ for a network operating in a Rayleigh block fading channel with blocklength $T_f = 1000$ and $\theta = 0.01$.

4.2. Interference cancellation via relaxation of delay constraint

In this section, we discuss how to compensate for the decrease in the per-user EC for the multiuser interference scenario by changing the value of delay constraint θ. More specifically, we try to determine the decrease in the value of θ and hence the delay bound extension needed to obtain the same EC_{max} as if the target user was transmitting without collision.

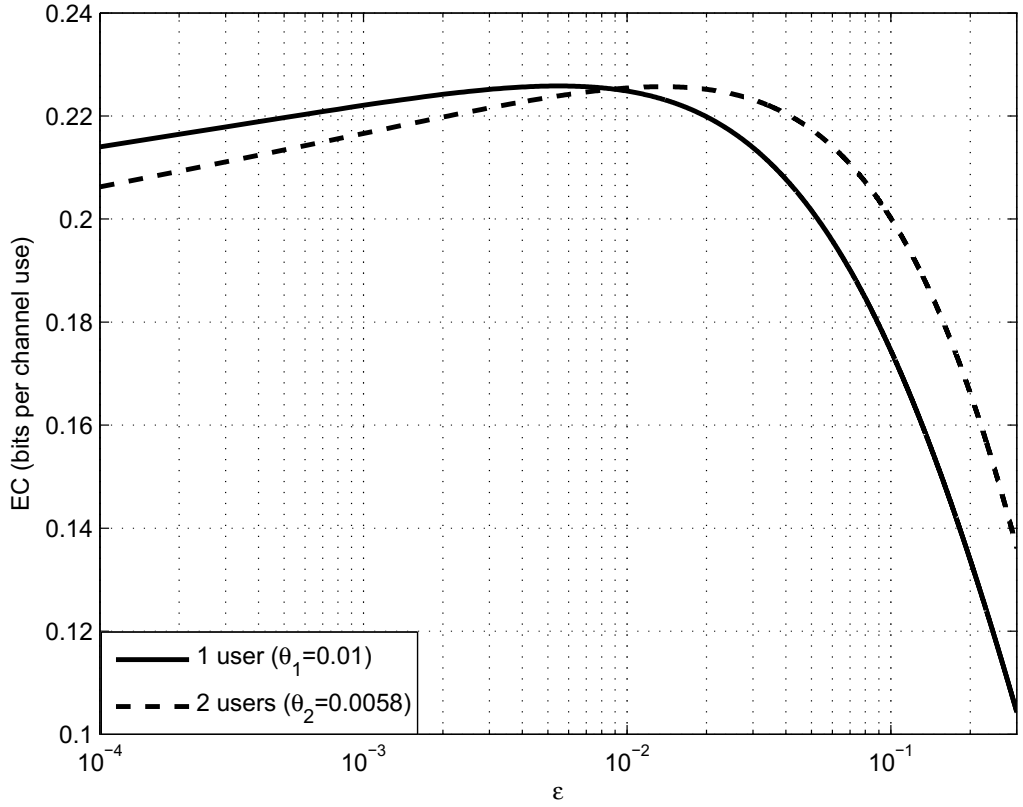

Figure 4.11. Interference cancellation via relaxation of delay constraint θ in case of 2 users colliding where $T_f = 1000$ and $\rho = 1$.

Let θ_1 be the original delay exponent in case of collision and θ_2 represent the new one, so our aim here is to equate the maximum effective capacity EC_{max} in the case of one and N users. This is formulated in (46)

$$EC_{Ry}(\rho, \theta_1, \epsilon^*) = EC_{Ry}(\rho_i, \theta_2, \epsilon_2^*) \tag{46}$$

$$\frac{-1}{T_f\theta_1} \log \left[\epsilon^* + (1-\epsilon^*) \int_0^\infty (1+\rho z)^{d_1} \sum_{n=0}^{2} \frac{(c_1 x_1)^n}{n!} e^{-z} dz \right]$$

$$= \frac{-1}{T_f\theta_2} \log \left[\epsilon_2^* + (1-\epsilon_2^*) \int_0^\infty (1+\rho_i z)^{d_2} \sum_{n=0}^{2} \frac{(c_2 x_2)^n}{n!} e^{-z} dz \right], \tag{47}$$

where

$$d_j = \frac{-\theta_j T_f}{\log 2},$$
$$c_j = \theta_j \sqrt{T_f} Q^{-1}(\epsilon_j^*) \log_2 e,$$
$$x_1 = \sqrt{(1 - \frac{1}{(1+\rho z)^2})},$$
$$x_2 = \sqrt{(1 - \frac{1}{(1+\rho_i z)^2})},$$

and ϵ_i^* is the maximizer of EC for the parameters (ρ, θ_1) and ϵ_2^* is the optimum error probability for (ρ_i, θ_2). Notice that (46) can be solved numerically to obtain the necessary value of θ_2 to compensate for the rate decrease due to collision in this case.

Applying (46) for a network of 2 users where $\theta_1 = 0.01$, $\rho = 1$ and $T_f = 1000$, we get $\theta_2 = 0.0058$. Thus, if we relax the delay constraint to 0.0058 instead of 0.01, we obtain the same value for the maximum effective capacity $EC_{max} = 0.226$. This corresponds to extending the maximum allowable delay D_{max} from 4100 to 5300 symbol periods with a delay outage probability of 10^{-3}. Note that the optimum error probabilities have different values in each case where $\epsilon_1^* = 0.0065$ and $\epsilon_2^* = 0.0122$. This is illustrated in Figure 4.11 where the compensated user has the same maximum EC in the two cases.

In contrary to the method of power control, the method of delay extension has a hidden advantage. It raises the EC without the need of extra power and this implicitly enhances the network service process and hence, the maximum delay bound for packets in the queue decreases. Thus, the relaxation of the delay exponent θ does not have a severe effect of the maximum delay bound. An example for this is depicted in the next section where we can see that the maximum delay remains almost the same before and after compensation.

4.3. Joint compensation via power control and relaxation of delay constraint

In this section, we discuss the trade off between compensation of interference effect via power control and via relaxation of delay constraint θ. We also propose a joint compensation of the decrease in EC using both power control and relaxation of delay constraint. For a certain user, a part of interference compensation can be done via power control and the rest can be performed by delay constraint relaxation. In this way, the degradation in EC of other users (set s) due to extra interference caused by power increase of the compensated user is less sharp. At the same time, the delay constraint is relaxed more gently, thus both side effects are less severe.

First, we start by defining the operational SINR in power controlled compensation for users in set s as ρ_{s_o} where ρ_{s_o} lies on the interval $[\rho_s\ \rho_i]$. Using (40), the operational SNR for the recovering user can be written as

$$\rho_{c_o} = \frac{\rho}{\rho_{s_o}} - 1 - \rho(N-2). \tag{48}$$

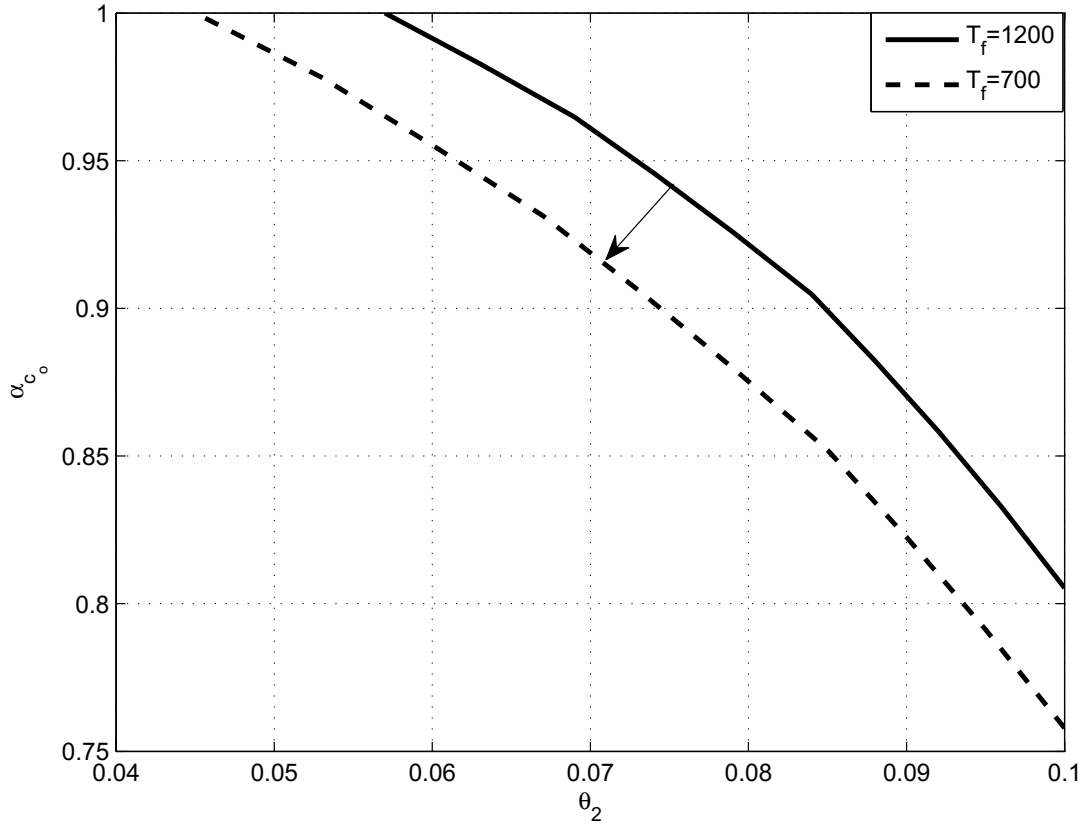

Figure 4.12. Trade off between compensation loss factor via power control α_{c_o} and relaxation of delay constraint θ_2 for different operational points.

The operational point of the compensation loss factor α_{c_o} is

$$\alpha_{c_o} = \frac{EC(\rho_{s_o}, \theta_1, \epsilon^*_{s_o})}{EC(\rho_i, \theta_1, \epsilon^*_i)}, \tag{49}$$

where $\epsilon^*_{s_o}$ is the optimum error probability obtained from (28) for the parameters (ρ_{s_o}, θ_1). α_{c_o} is considered to be the loss factor caused by the part of compensation performed via power control.

After that, we perform the rest of compensation via relaxation of θ as in Section 4.2. Our aim here is to equate the maximum EC in the case of one user alone and the same user when present as a part of N users after partial compensation via power control. That is

$$EC_{Ry}(\rho, \theta_1, \epsilon^*) = EC_{Ry}(\frac{\rho_{c_o}}{1+\rho(N-1)}, \theta_2, \epsilon^*_2) \tag{50}$$

$$\frac{-1}{T_f\theta_1} \log \left[\epsilon^* + (1-\epsilon^*) \int_0^\infty (1+\rho z)^{d_1} \sum_N \frac{(c_1 x_1)^n}{n!} e^{-z} dz \right]$$

$$= \frac{-1}{T_f\theta_2} \log \left[\epsilon^*_2 + (1-\epsilon^*_2) \int_0^\infty (1+\frac{\rho_{c_o}}{1+\rho(N-1)} z)^{d_2} \sum_N \frac{(c_2 x_2)^n}{n!} e^{-z} dz \right]. \tag{51}$$

From (51), we can conclude the necessary value of θ_2 to continue the compensation process via delay relaxation.

Figure 4.12 illustrates different operational points for interference compensation for different blocklength T_f where the system parameters are set as $N = 5$, $\rho = 1$, $P_{out\_delay} = 10^{-3}$ and $\theta_1 = 0.1$. For example, when $T_f = 700$, we select the operational point $\alpha_{c_o} = 0.9, \theta_2 = 0.075$. This means that a part of compensation for the user under consideration will be performed via power control which leads to a 0.9 loss in EC of other users (set s). Then the rest of compensation will be performed by relaxing its θ from 0.1 to 0.075. Here is an example of how the restoration of EC compensates for the decrease in delay exponent where the maximum delay of the recovering user remains 2500 symbol periods before and after recovery as in (5). The figure also shows that for shorter packets, the amount of compensation needed by both θ relaxation and power increase is higher when a point is moved to the new curve. Thus, it is more costly to compensate networks transmitting shorter packets.

It is simple to implement joint compensation by selecting any operational point on the curve. However, here a question triggers one's mind: which operational point should we choose and according to which criteria ?

To characterize this, we propose an objective function leveraging the system performance in case of hybrid compensation via power control and relaxation of θ according to network design preferences. Let us define the priority factor η_α as a measure of the risk implied by the decrease in EC of users in set s when the compensating user boosts its transmission power. In other words, the higher the value of η_α, the more important it is for user in set s to maintain their ECs and hence, we try not to compensate via power control and shift compensation towards θ relaxation. On the other hand, we define the priority factor η_θ as a measure of strictness of the delay constraint (i.e., the higher the value of η_θ, the more strict it is not to change delay constraint and hence, the less we are allowed to relax θ to get higher EC for the compensating user). Note that as the value of θ_2 gets lower, the delay bound is raised which is not feasible for delay critical applications. Priority factors can be chosen to be any non-negative values. Thus we can formalize our objective function as the summation

$$\eta = \eta_\alpha \alpha_{c_o} + \eta_\theta \theta_2 \tag{52}$$

where (α_{c_o}, θ_2) is the operational point and $\alpha_{c_o} \in [0, 1]$. Now, we choose this operational point to satisfy

$$\begin{aligned} \eta_{max} = &\max_{\theta_2 \geq 0} \ \eta_\alpha \alpha_{c_o} + \eta_\theta \theta_2, \\ &s.t \ \ \rho_s \leq \rho_{s_o} \leq \rho_i. \end{aligned} \tag{53}$$

where the solution to this problem gives the optimum operational point which can be found from (48), (49) and (50).

According to the system parameters, certain values of the priority factors η_α and η_θ may produce a concave maximization problem for the objective function η. This is illustrated in Figure 4.13 for $N = 15, T_f = 1000, \rho = 2, \theta_1 = 0.1, \eta_\alpha = 1$ and $\eta_\theta = 4$. The optimum value of ρ_{s_o} in this case is 0.057 which corresponds to the operational point $\alpha_{c_o} = 0.9397$ and $\theta_2 = 0.053$. The SNR of the recovering user becomes $\rho_{c_o} = 8.08$. In other words, in order to maximize the system throughput according to the given priority factors, the compensating user boosts its SNR from 2 to 8.08 and relaxes its delay exponent from 0.1 to 0.053 which results in 6% loss in EC of other users. This is depicted in Figure 4.14. Priority factors are left for the designer's preferences depending on reliability or latency requirements.

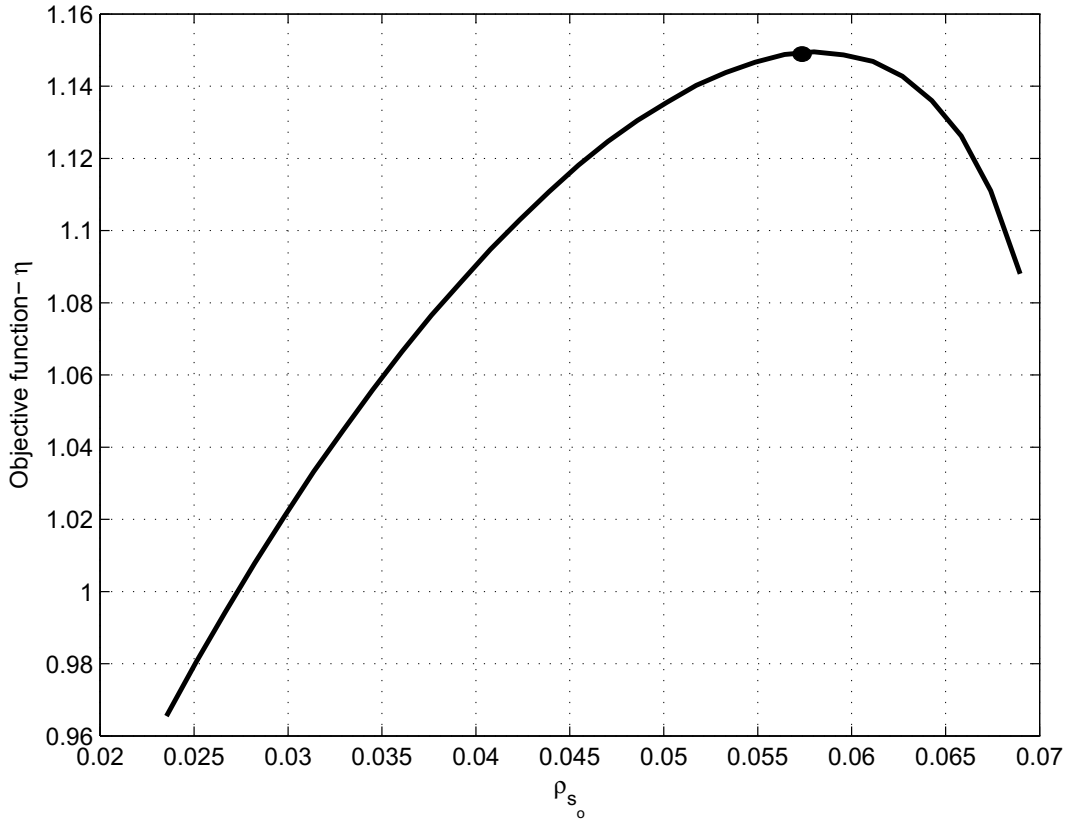

Figure 4.13. η for $T_f = 1000, \theta = 0.1, \rho = 2$, and $N = 15$.

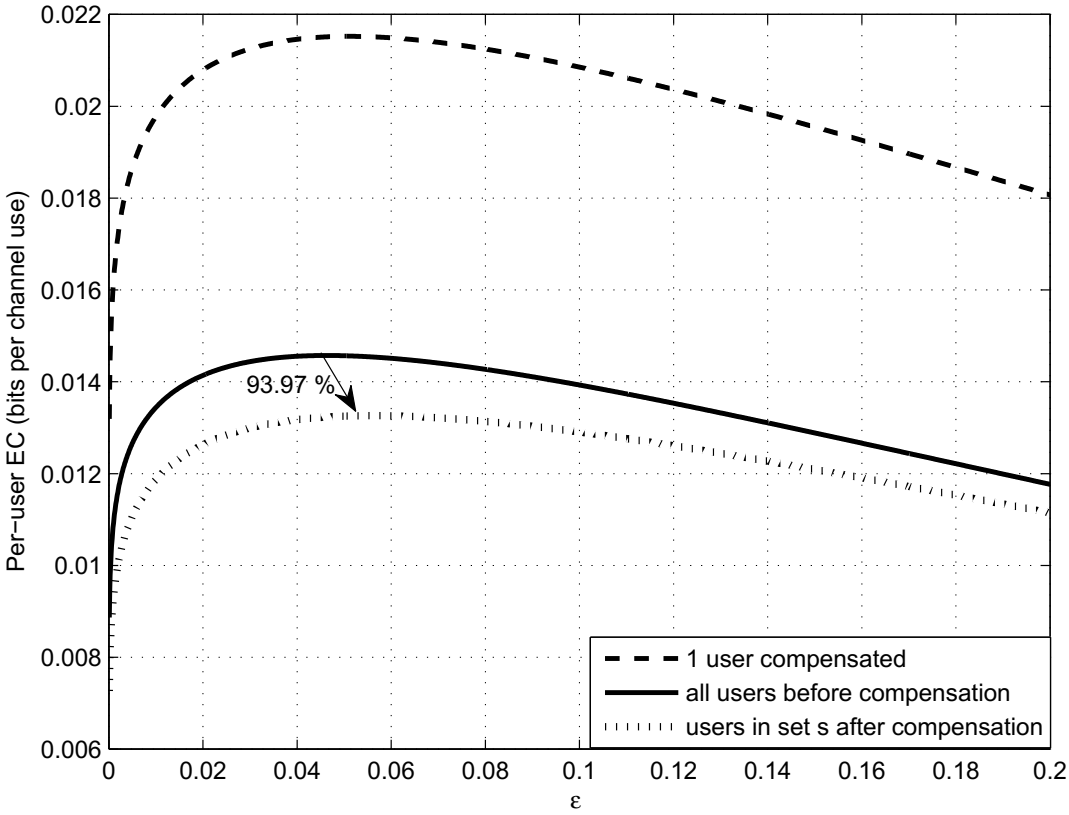

Figure 4.14. Per-user EC as a function of error probability ϵ before and after hybrid compensation for $T_f = 1000, \theta_1 = 0.1, \rho = 2$, and $N = 15$.

5. EFFECTIVE ENERGY EFFICIENCY ANALYSIS

As discussed in the previous chapter, the raise of transmission power boosts the EC but at the cost of energy consumption which is not feasible for energy limited systems such as smart grids, vehicular networks, and massive machine to machine type systems which are the main concern of our analysis. Such networks are usually isolated from stationary power sources and thus they are energy limited. Now that we have characterized the per-node EC and the trade-offs implied by interference alleviation, we need to study the energy consumption of such networks and the trade-off between the per-user EC and the per-user EEE.

In this section, we discuss the per-user EEE in FB regime for different power models. Previously, we assumed that the buffer is always full which practically is not always the case. In real transmission, there would be instants in which a certain user becomes idle and therefore has no data to transmit. Thus, we need to account for the case the buffer is empty as was considered in [34]. We extend the results obtained in [34] to multi-user networks operating in the FB regime with non-vanishing probability of error ϵ. We investigate the effect of EEE maximization with empty buffer probability and compare it with the case of always full buffer. After accounting for a non-empty buffer probability which is equal to (1-probability of empty buffer), the per-user power consumption is formulated as

$$P_t(p) = P_{nb}\zeta p + P_c = \frac{\mu}{r}\zeta\rho + P_c, \tag{54}$$

with $P_{nb} = \mu/r$ is the non-empty buffer probability (NBP) which has a value of 1 if the buffer is considered to be always full. In this case, the per-user EEE is given by

$$EEE = \frac{-\frac{1}{T_f\theta}\log\left(E_{z=|h|^2}\left[\epsilon + (1-\epsilon)e^{-T_f\theta r}\right]\right)}{\frac{\mu}{E[r]}\zeta\rho + P_c}, \tag{55}$$

where the numerator represents the effective capacity EC in the finite blocklength regime. It is worth mentioning that here we consider NBP only for one user (the user under consideration). Therefore, P_{nb} is not affecting the rate calculation of other nodes and ρ_i. In future work, we plan to consider NBP for all users.

5.1. Verifying the EEE model with empty buffer probability in FB

It was proven in [34] that the power consumption model considering the probability of empty buffer fulfills the characteristic properties of an energy efficiency function mentioned in [32] for the Shannon Capacity model. An energy efficiency function must be non-negative, must be zero when the transmit power is zero, and must tend to zero as the transmit power tends to infinity. Here, we start by verifying that this power consumption model is valid for the blocklength limited EC model.

Lemma 2. *The EEE in (55) is zero for $\rho = 0$ and tends to 0 when $\rho \to \infty$.*

Proof. For $\rho = 0$, the achievable rate $r = 0$ and the numerator of (55) becomes 0. Applying L'Hopital's rule for the denominator, we have

$$\lim_{\rho\to 0}\frac{\rho}{r} = \lim_{\rho\to 0}\frac{1}{z\left(\frac{1}{(1+\rho_i z)\log 2} - \frac{Q^{-1}(\epsilon)\log_2(e)}{\sqrt{T_f}(1+\rho_i z)^3 x}\right)(1+\rho(N-1))^2} = 0. \tag{56}$$

Thus the denominator of (55) equals to P_c yielding 0 for the EEE.

For the second condition, (17) implies that $\lim_{\rho\to\infty}\rho_i = \frac{1}{N-1}$ and Hence, from (4), we can infer that r is a finite function of the number of users N while the denominator of (55) tends to ∞. Thus the EEE vanishes. The validity of the EEE expression in (55) is verified in the FB regime. □

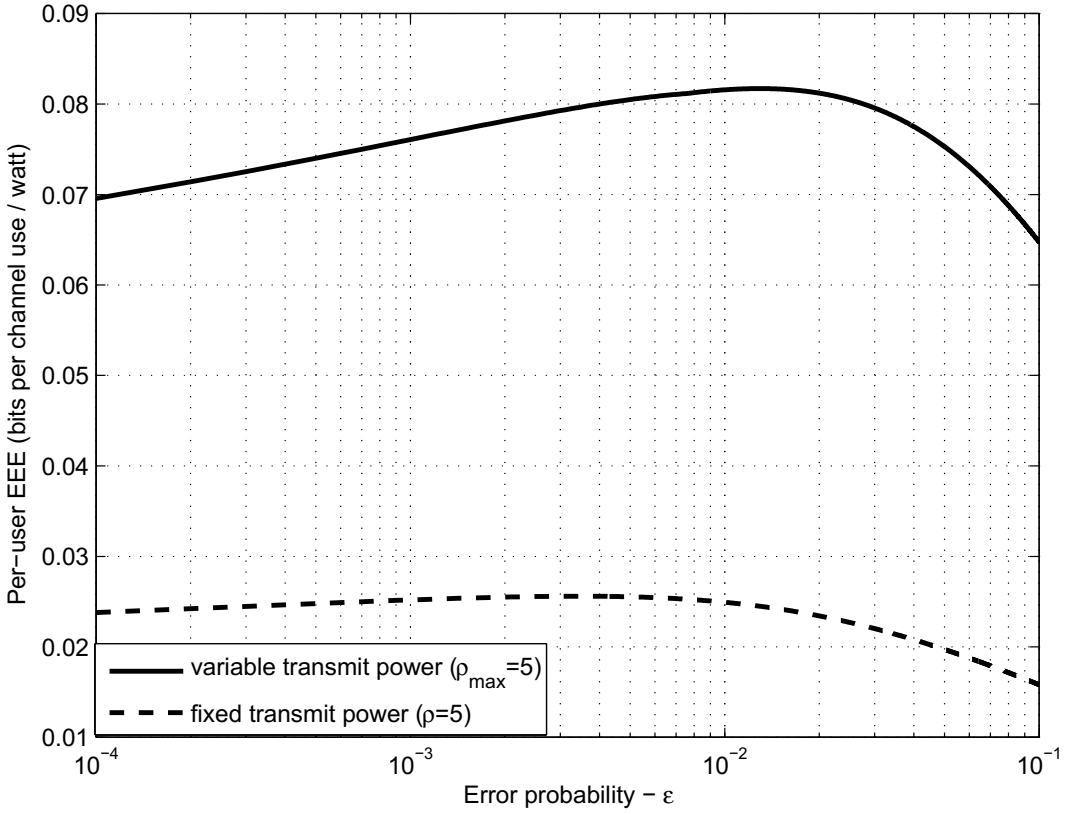

Figure 5.1. EEE vs ϵ with and variable transmit power ρ for $N = 2, P_{out\_delay} = 10^{-2}, P_c = 0.2, \zeta = 0.2, \mu = 0.2, D_{max} = 200$, and $T_f = 1000$.

5.2. EEE maximization with buffer constraints

We investigate the per-user EEE maximization with EC, delay, and power constraints. EC should be higher than the arrival rate μ to guarantee a stable queue while the transmission SNR ρ has a higher bound ρ_{max}. Thus, the optimization problem is formulated as

$$\begin{aligned} \max_{\rho\geq 0,\theta\geq 0} \quad & \frac{-\frac{1}{T_f\theta}\log\left[\epsilon+(1-\epsilon)\int_0^\infty(1+\rho_i z)^d\sum_{n=0}^{2}\frac{(cx)^n}{n!}e^{-z}dz\right]}{\frac{\mu}{r}\zeta\rho+P_c}, \\ s.t \quad & EC(\rho_i,\theta,\epsilon)\geq\mu \\ & P_b e^{-\theta\mu D_{max}}\leq P_{out\_delay} \\ & \rho\leq\rho_{max}. \end{aligned} \tag{57}$$

Here P_{out_delay} is the maximum allowed delay outage probability. The optimal value of θ can be obtained from the second constraint as

$$\theta^*(\rho)=\frac{1}{\mu D_{max}}log\frac{\mu}{P_{out\_delay}E_z\left[R_s\right]}. \tag{58}$$

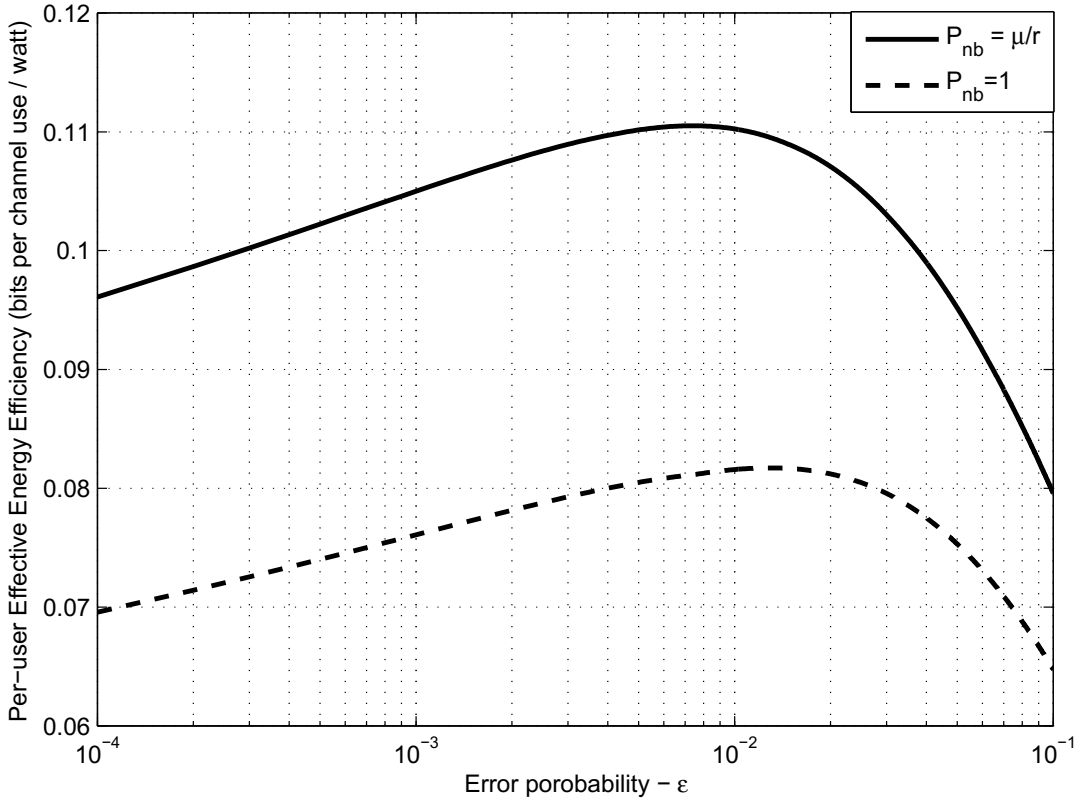

Figure 5.2. Per-user EEE vs ϵ with and without empty-buffer probability for $N=2, P_{out\_delay}=10^{-2}, P_c=0.2, \zeta=0.2, \mu=0.2, D_{max}=200$, and $T_f=1000$.

We plot the maximum per-user EEE as a function of error outage probability ϵ for fixed and variable transmit power ρ in Figure 5.1 for the parameters $P_{out\_delay}=$

$10^{-2}, P_c = 0.2, \zeta = 0.2, \mu = 0.2, D_{max} = 200, \rho = 5$ (fixed case), $\rho_{max} = 5$, and $T_f = 500$. In case of variable transmission power, we notice that the per-user EEE is higher than the case of fixed ρ. This is because the system selects the optimum value of ρ which maximizes the EEE in each iteration of ϵ. Thus, we can obtain the favorable value of ϵ and ρ for maximizing the per-user EEE in both variable and fixed transmit power scenarios.

Furthermore, in Figure 5.2, we include a plot for the EEE in case of empty buffer probability and compare it to the case where the buffer is always full. The system parameters are the same as Figure 5.1 with $\rho_{max} = 5$ (variable transmission power). Here, the advantage of considering empty buffer probability is two fold. It is clear that non empty buffer allows for a better modeling of the power consumption, thus is a more realistic model. This reflects that full buffer is the worst case, where we assume that all power will be consumed while non empty models the fraction that is actually used according to queue congestion which highlights the gain of this model compared to always full buffer. Moreover, the optimum error probability ϵ^* for maximizing the per-user EEE is lower when considering empty buffer probability.

Figure 5.3 depicts the achieved per-user EEE for different delay limits D_{max} and the same network parameters as in the previous two figures. We observe that the per-user EEE increases when increasing D_{max} and the delay outage probability P_{out_delay}. Also, considering empty buffer probability significantly boosts the per-user EEE.

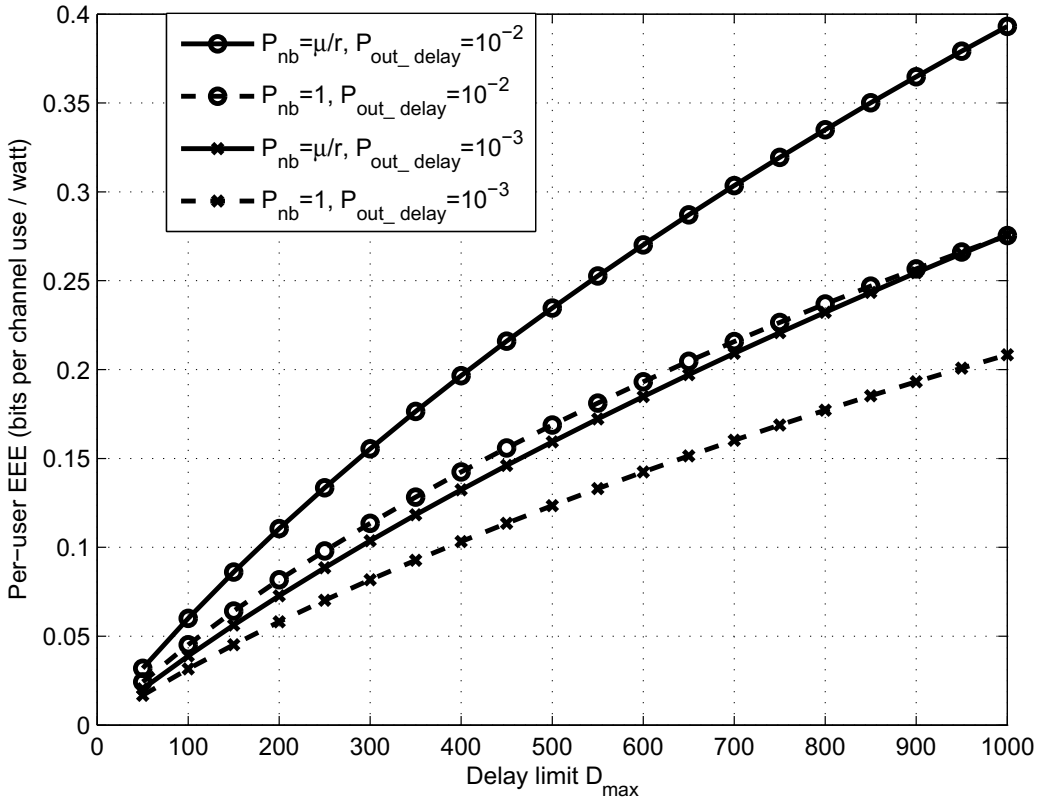

Figure 5.3. Per-user EEE vs D_{max} with and without empty-buffer probability for $N = 2, P_{out\_delay} = 10^{-2}, 10^{-3}, P_c = 0.2, \zeta = 0.2, \mu = 0.2$, and $T_f = 1000$.

6. CONCLUSIONS

In this work, we presented a detailed analysis of the performance of delay constrained multi-user networks in the finite blocklength regime. First, we offered a literature review for FB communication in Chapter 2. For Rayleigh fading collision channels, we obtained a closed form for the per-user EC and investigated the effect of interference on the per-user EC in Chapter 3. In Chapter 4, we suggested three methods to compensate for this collision effect. The first technique is power control where one of the users is allowed to raise its transmission power which causes more interference to other users in return. Power control is shown to be more suitable for systems with less stringent delay constraints. The second method is relaxation of delay constraint. Joint compensation emerges as a combination between these two methods where an operational point is selected to maximize an objective function according to the system design aspects. The results of implementing this method showed that for shorter packets, the amount of compensation needed by both θ relaxation and power increase is higher when a point is moved to the new curve. Thus, it is more costly to compensate networks transmitting shorter packets.

Our analysis was not limited only to the EC as we also explored the EEE of such networks Chapter 5. We showed that considering non-empty buffer probability and flexible transmission power significantly improves the per-user EEE of multi-user networks operating in the FB regime. We investigated the trade off between EEE and maximum delay limit D_{max}. The results show that allowing for larger delays significantly boosts the per-user EEE.

In future work, we are looking to analyze the EC-error trade-off discussed in Chapter 3 and look for an analytical solution to optimum error probability ϵ. We also suggest considering empty buffer probability for all nodes in a game theoretic model to maximize EEE and EC.

7. REFERENCES

[1] C. E. Shannon, “A mathematical theory of communication,” *The Bell System Technical Journal*, vol. 27, no. July 1928, pp. 379–423, 1948. [Online]. Available: http://cm.bell-labs.com/cm/ms/what/shannonday/shannon1948.pdf

[2] G. Durisi, T. Koch, and P. Popovski, “Toward Massive, Ultrareliable, and Low-Latency Wireless Communication with Short Packets,” *Proceedings of the IEEE*, vol. 104, no. 9, pp. 1711–1726, 2016.

[3] M. C. Gursoy, “Throughput analysis of buffer-constrained wireless systems in the finite blocklength regime,” *IEEE International Conference on Communications*, pp. 1–13, 2011.

[4] P. Popovski, “Ultra-Reliable Communication in 5G Wireless Systems,” *CoRR*, vol. abs/1410.4, pp. 4–9, 2014. [Online]. Available: http://arxiv.org/abs/1410.4330

[5] Q. Zhang and F. H. P. Fitzek, “Mission Critical IoT Communication in 5G,” in *Future Access Enablers for Ubiquitous and Intelligent Infrastructures*, V. Atanasovski and A. Leon-Garcia, Eds. Springer International Publishing, 2015, vol. 159, pp. 35–41. [Online]. Available: http://link.springer.com/10.1007/978-3-319-27072-2

[6] S. Andreev, O. Galinina, A. Pyattaev, M. Gerasimenko, T. Tirronen, J. Torsner, J. Sachs, M. Dohler, and Y. Koucheryavy, “Understanding the IoT connectivity landscape: a contemporary M2M radio technology roadmap,” *IEEE Communications Magazine*, vol. 53, no. 9, pp. 32–40, sep 2015. [Online]. Available: http://ieeexplore.ieee.org/lpdocs/epic03/wrapper.htm?arnumber=7263370

[7] 3GPP, “3GPP TR 22.861:Technical Specification Group Services and System Aspects; Feasibility Study on New Services and Markets Technology Enablers for Massive Internet of Things;,” *Rel 14*, vol. 14.0.0, p. 28, 2016.

[8] M. Park, “IEEE 802.11ah: sub-1-GHz license-exempt operation for the internet of things,” *IEEE Communications Magazine*, vol. 53, no. 9, pp. 145–151, sep 2015. [Online]. Available: http://ieeexplore.ieee.org/lpdocs/epic03/wrapper.htm?arnumber=7263359

[9] Nokia, “5G Masterplan - fice keys to create the new communications era,” Tech. Rep., 2016.

[10] N. a. Johansson, Y.-P. E. Wang, E. Eriksson, and M. Hessler, “Radio access for ultra-reliable and low-latency 5G communications,” in *2015 IEEE International Conference on Communication Workshop (ICCW)*. IEEE, jun 2015, pp. 1184–1189. [Online]. Available: http://ieeexplore.ieee.org/lpdocs/epic03/wrapper.htm?arnumber=7247338

[11] M. Simsek, A. Aijaz, M. Dohler, J. Sachs, and G. Fettweis, "5G-Enabled Tactile Internet," *IEEE Journal on Selected Areas in Communications*, vol. 34, no. 3, pp. 460–473, mar 2016. [Online]. Available: http://ieeexplore.ieee.org/lpdocs/epic03/wrapper.htm?arnumber=7403840

[12] Nokia, "5G for Mission Critical Communication: Achieve ultra-reliability and virtual zero latency," *Nokia White Paper*, 2016.

[13] A. Ali, W. Hamouda, and M. Uysal, "Next generation M2M cellular networks: challenges and practical considerations," *IEEE Communications Magazine*, vol. 53, no. 9, pp. 18–24, sep 2015.

[14] I. Stojmenovic, "Machine-to-Machine Communications With In-Network Data Aggregation, Processing, and Actuation for Large-Scale Cyber-Physical Systems," *IEEE Internet of Things Journal*, vol. 1, no. 2, pp. 122–128, 2014. [Online]. Available: http://ieeexplore.ieee.org/lpdocs/epic03/wrapper.htm?arnumber=6766661

[15] T. Adame, A. Bel, B. Bellalta, J. Barcelo, and M. Oliver, "IEEE 802.11AH: the WiFi approach for M2M communications," *IEEE Wireless Communications*, vol. 21, no. 6, pp. 144–152, dec 2014. [Online]. Available: http://ieeexplore.ieee.org/lpdocs/epic03/wrapper.htm?arnumber=7000982

[16] H. Shariatmadari, S. Iraji, and R. Jantti, "Analysis of transmission methods for ultra-reliable communications," *IEEE International Symposium on Personal, Indoor and Mobile Radio Communications, PIMRC*, vol. 2015-Decem, pp. 2303–2308, 2015.

[17] J. J. Nielsen and P. Popovski, "Latency analysis of systems with multiple interfaces for ultra-reliable M2M communication," in *2016 IEEE 17th International Workshop on Signal Processing Advances in Wireless Communications (SPAWC)*. IEEE, jul 2016, pp. 1–6. [Online]. Available: http://ieeexplore.ieee.org/lpdocs/epic03/wrapper.htm?arnumber=7536857

[18] W. Yang, G. Durisi, T. Koch, and Y. Polyanskiy, "Block-Fading Channels at Finite Blocklength," *Proceedings of the Tenth International Symposium on Wireless Communication Systems (ISWCS 2013)*, vol. 9, pp. 410–413, 2013.

[19] R. Devassy, G. Durisi, P. Popovski, and E. G. Strom, "Finite-blocklength analysis of the ARQ-protocol throughput over the Gaussian collision channel," *ISCCSP 2014 - 2014 6th International Symposium on Communications, Control and Signal Processing, Proceedings*, pp. 173–177, 2014.

[20] Y. Hu, J. Gross, and A. Schmeink, "On the Capacity of Relaying with Finite Blocklength," *IEEE Transactions on Vehicular Technology*, vol. 65, no. 3, pp. 1790–1794, 2016.

[21] Y. Hu, A. Schmeink, and J. Gross, "Blocklength-limited performance of relaying under quasi-static rayleigh channels," *CoRR*, vol. abs/1602.02924, 2016.

[22] S. Schiessl, H. Al-Zubaidy, M. Skoglund, and J. Gross, "Analysis of Wireless Communications with Finite Blocklength and Imperfect Channel Knowledge," *arXiv*, pp. 1–30, 2016.

[23] M. Gursoy, "Throughput analysis of buffer-constrained wireless systems in the finite blocklength regime," in *EURASIP Journal on Wireless Communucations and Networking 2013*, 2013.

[24] W. Yang, G. Durisi, T. Koch, and Y. Polyanskiy, "Diversity versus channel knowledge at finite block-length," in *2012 IEEE Information Theory Workshop, Lausanne, Switzerland, September 3-7, 2012*, 2012, pp. 572–576. [Online]. Available: http://dx.doi.org/10.1109/ITW.2012.6404740

[25] Y. Li, G. Ozcan, M. C. Gursoy, and S. Velipasalar, "Energy efficiency of hybrid-arq under statistical queuing constraints," *IEEE Trans. Communications*, vol. 64, no. 10, pp. 4253–4267, 2016. [Online]. Available: http://dx.doi.org/10.1109/TCOMM.2016.2599109

[26] Y. Li, M. C. Gursoy, and S. Velipasalar, "On the throughput of hybrid-arq under statistical queuing constraints," *IEEE Trans. Vehicular Technology*, vol. 64, no. 6, pp. 2725–2732, 2015. [Online]. Available: http://dx.doi.org/10.1109/TVT.2014.2342154

[27] J. Park and D. Park, "A new power allocation method for parallel AWGN channels in the finite block length regime," *IEEE Communications Letters*, vol. 16, no. 9, pp. 1392–1395, 2012. [Online]. Available: http://dx.doi.org/10.1109/LCOMM.2012.071612.120447

[28] D. Wu and R. Negi, "Effective capacity: a wireless link model for support of quality of service," *IEEE Trans. Wireless Commun*, vol. 2, no. 4, pp. 630–643, 2003.

[29] C. Bockelmann, N. Pratas, H. Nikopour, K. Au, T. Svensson, C. Stefanovic, P. Popovski, and A. Dekorsy, "Massive Machine-Type Communications in 5G : Physical and MAC-Layer Solutions," *IEEE Communications Magazine*, no. September, pp. 59–65, 2016.

[30] C. Goursaud and J. M. Gorce, "Dedicated networks for IoT: PHY / MAC state of the art and challenges," *EAI Endorsed Transactions on Internet of Things*, vol. 1, no. 1, oct 2015. [Online]. Available: http://eudl.eu/doi/10.4108/eai.26-10-2015.150597

[31] L. Musavian and T. Le-Ngoc, "QoS-based power allocation for cognitive radios with AMC and ARQ in Nakagami-m fading Channels," in *Trans. Emerging Tel. Tech.*, vol. 27, 2014, pp. 266–277.

[32] A. Zappone and E. Jorswieck, *Digital Communication over Fading Channels: A Unified Approach to Performance AnalysisEnergy efficiency in wireless networks via fractional programming theory*. Found. Trends Commun. Inf. Theory,, 2015, vol. 11.

[33] A. Laya, L. Alonso, P. Chatzimisios, and J. Alonso-Zarate, "Massive access in the Random Access Channel of LTE for M2M communications: An energy perspective," in *2015 IEEE International Conference on Communication Workshop (ICCW)*. [Online]. Available: http://ieeexplore.ieee.org/lpdocs/epic03/wrapper.htm?arnumber=7247383

[34] M. Sinaie, A. Zappone, E. A. Jorswieck, and P. Azmi, "A Novel Power Consumption Model for Effective Energy Efficiency in Wireless Networks," *IEEE Wireless Communications Letters*, vol. 5, no. 2, pp. 152–155, 2016.

[35] L. Musavian, Q. Ni, and S. Member, "Effective Capacity Maximization With Statistical Delay and Effective Energy Efficiency Requirements," vol. 14, no. 7, pp. 3824–3835, 2015.

[36] C. She and C. Yang, "Energy Efficiency and Delay in Wireless Systems: Is Their Relation Always a Tradeoff?" *IEEE Transactions on Wireless Communications*, vol. 15, no. 11, pp. 7215–7228, 2016. [Online]. Available: http://ieeexplore.ieee.org/document/7539651/

[37] N. Petreska, H. Al-Zubaidy, R. Knorr, and J. Gross, "Power-Minimization under Statistical Delay Constraints for Multi-Hop Wireless Industrial Networks," *arXiv*, 2016. [Online]. Available: http://arxiv.org/abs/1608.02191

[38] J. Scarlett, V. Y. F. Tan, and G. Durisi, "The dispersion of nearest-neighbor decoding for additive non-gaussian channels," *CoRR*, vol. abs/1512.06618, 2015. [Online]. Available: http://arxiv.org/abs/1512.06618

[39] M.-S. A. Marvin K. Simon, *Digital Communication over Fading Channels: A Unified Approach to Performance Analysis*. Copyright 2000 John Wiley & Sons, Inc., 2005.